

THEORY OF GAS EXCHANGE IN THE AVIAN LUNG

by

WILLIAM DAVID CRANK

B.S., Kansas State University, 1968

A MASTER'S THESIS

submitted in partial fulfillment of the

requirements for the degree

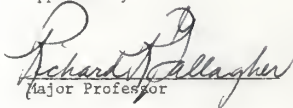
MASTER OF SCIENCE

Department of Electrical Engineering

KANSAS STATE UNIVERSITY
Manhattan, Kansas

1978

Approved by:


Major Professor

Document +
LD
2668
T4
1978
C 73
C 2

TABLE OF CONTENTS

	Page
I. INTRODUCTION	1
II. THE MODEL	4
III. DERIVATION OF DIFFERENTIAL EQUATIONS	9
3.1 The Air Capillary-Blood Capillary Pair	9
3.2 The Parabronchus	13
IV. SOLUTION OF DIFFERENTIAL EQUATIONS	19
4.1 Case 1	20
4.2 Case 2	22
4.3 Case 3	29
4.4 Case 4	35
4.5 Case 5	38
V. PARAMETERS OF THE MODEL	44
5.1 Physical Parameters of the Lung	44
5.2 Blood Parameters	47
5.3 Diffusing Capacity of the Lung	49
5.4 Gas Parameters	49
5.5 Ventilation and Cardiac Output	50
VI. RESULTS AND DISCUSSION	51
VII. RECOMMENDATIONS FOR FUTURE WORK	73
REFERENCES	76
APPENDIX A. Definitions of Symbols	A1
APPENDIX B. Publication Manuscript	B1

LIST OF FIGURES

Figure		Page
1.	A: The parabronchial model. B: Detail of air capillary and blood capillary compartments. C: Detail of parabronchial luminal compartments	6
2.	Single compartment composed of a segment of a blood-air capillary pair	12
3.	Single compartment defined by two cross-sectional cuts through the parabronchus	16
4.	Geometrical relationship of pre-parabronchial, parabronchial, and post-parabronchial regions	26
5.	Simulation diagram	30
6.	Oxygen dissociation curve, linear approximation to it, and 2nd degree polynomial approximation to it	39
7.	Fractional distribution of lung volume in domestic fowl	44
8.	Partial pressures along a blood capillary and an air capillary. A: P_{O_2} along the blood capillary. B: P_{O_2} along the air capillary. C: P_{CO_2} along the blood capillary. D: P_{CO_2} along the air capillary	52
9.	Partial pressures along the parabronchus. A: P_{O_2} . B: P_{CO_2}	55
10.	A: O_2 partial pressure along several parabronchial blood capillaries and along the parabronchial lumen. B: CO_2 partial pressure along several parabronchial blood capillaries and along the parabronchial lumen . . .	58
11.	O_2 partial pressures along blood capillaries and parabronchus computed with a non-linear dissociation curve. Cardiac output = 234 ml/min; ventilation = 360 ml/min	60
12.	O_2 partial pressures along blood capillaries and parabronchus computed with a non-linear dissociation curve. Cardiac output = 1170 ml/min; ventilation = 1800 ml/min	61

LIST OF FIGURES (Continued)

Figure		Page
13.	O_2 concentrations along blood capillaries computed with a non-linear dissociation curve. A: Cardiac output = 234 ml/min; ventilation = 360 ml/min. B: Cardiac output = 1170 ml/min; ventilation = 1800 ml/min	63
14.	Dependence of end-parabronchial O_2 partial pressure on cardiac output and ventilation	66
15.	Dependence of arterial O_2 partial pressure on cardiac output and ventilation	67
16.	Dependence of arterial O_2 concentration on cardiac output and ventilation	68
17.	Dependence of O_2 uptake on cardiac output and ventilation	69
18.	Upper limit on O_2 uptake by the lungs as a function of venous O_2 partial pressure	71

I. INTRODUCTION

A model of gas exchange in the avian lung is developed. The physical structure of the model is based upon that proposed by Zeuthen [1]. Differential equations are derived to describe the function of the model. In addition to gas transfer between blood and air which occurs across the exchange surfaces of the lung and gas movement by bulk flow through the lung, the mathematical description of the function of the model also accounts for movement of a gas component through the air spaces of the lung by diffusion. Cases which treat diffusion in the air capillaries, diffusion in the parabronchial lumen, and diffusion in both these spaces are considered. In those cases which describe diffusion through the air spaces, the dissociation curve relating concentration and partial pressure in the blood is linear. Another case has been considered in which the diffusion through the air spaces is neglected, but a more accurate representation of the non-linear oxygen dissociation curve is made. By approximating that curve as a polynomial of second or third order, integration of the differential equations describing gas transfer between air and blood capillaries can still be accomplished. This latter technique, although applied here to the avian lung, might also find application in analysis of gas transfer between pulmonary capillaries and the alveoli of mammalian lungs. With diffusion not accounted for, and with a linear dissociation curve, the model can be shown to be equivalent to that of Scheid and Piiper [2].

Solutions of the differential equations are evaluated and the results displayed graphically. Under different conditions of cardiac output and ventilation the partial pressure profiles of oxygen and carbon dioxide in the blood capillaries, air capillaries, and parabronchial lumen are

displayed. The cases of diffusion and no diffusion are contrasted. The case of the model with a non-linear dissociation curve has also been utilized to briefly analyze performance of oxygen uptake by the lung.

The effort which resulted in the avian lung model presented in this thesis originally arose out of a speculation on how to determine possible locations for the CO_2 receptors (see reference [3] for a description of these receptors) which are present in the avian lung. Single unit recordings from the vagus nerve yield information about the CO_2 partial pressure in the microenvironment of the receptors themselves. If a correspondence could be established between CO_2 partial pressures and various locations within the lung under given conditions of cardiac output, ventilation, and partial pressure in the venous blood and inspired gas, then the possible locations could be mapped out. Considerable economy of effort would be achieved by confining the search for these receptors to the indicated regions.

The function of the model is based upon a parabronchial structure which contains a representation of air capillaries and blood capillaries in addition to the lumen, since the receptors might be located within any of these structures. Since the physical dimensions of air capillaries, blood capillaries, and parabronchial lumina are so small that experimental measurements of partial pressure cannot be made within them, a mathematical model provides a method of determining their partial pressures.

The actual determination of possible locations for the CO_2 receptors has not been performed, since the experimental results which have been published are not in a form which allows comparison with the results of the model.

The form in which the model was initially developed is that presented in Cases 1, 2, 3, 4 of Chapter IV. As computations were made it became

apparent that the assumption of a linear dissociation curve, although valid for carbon dioxide, was resulting in unrealistic results for oxygen exchange. So a secondary objective became the development of a simple, yet reasonably accurate, way of incorporating the sigmoid dissociation curve of oxygen into the model. This objective was met. The solution is Case 5 of Chapter IV.

II. THE MODEL

The mathematical model which is developed here is fundamentally a model of the avian parabronchus. It is assumed that several hundred of these parabronchi, all identical, function "in parallel" to make up the avian lung. These parabronchi are all to be of identical structure, to receive identical flows of blood and gas which enter the parabronchi at identical compositions. This is an accurate representation of the paleopulmo, but not of the neopulmo, which is composed of parabronchi of widely varying lengths. But since the neopulmo, when present, makes up a small fraction of the lung, exceeding 25% in no species, it is perhaps not unreasonable to assume the paleopulmonic construction for the whole lung. Assuming no blood is shunted past the lung, the rate of blood flow to a single parabronchus is given by the cardiac output divided by the number of parabronchi. The ventilation of an individual parabronchus is assumed to be given by the minute ventilation divided by the number of parabronchi. This implies that all the gas included in the figure for minute ventilation makes one pass through a parabronchus.

In a bird the parabronchus is basically a cylindrical structure which is penetrated by a lumen along its central axis. Ventilated gas passes down the lumen. Along the wall of the lumen are many small, transverse bands of smooth muscle which define the walls of air pockets termed "atria". The atria open into the lumen, and evaginating radially outward from them are many air capillaries. Coursing adjacent to the air capillaries are the blood capillaries. The direction of blood flow in these is from the arterioles at the outer periphery of the parabronchus inward toward the venules located adjacent to the lumen. Surrounding the parabronchial lumen, this network of air and blood capillaries together makes up the parabronchial

mantle. It is in the mantle, across the surfaces separating blood from gas that oxygen and carbon dioxide exchange takes place. For a detailed description of avian lung anatomy, see Dunker [4,5].

The physical structure of the model which is to represent the actual parabronchus is illustrated in Figure 1A. This representation in essence is due originally to Zeuten [1]. In it the detailed structure of smooth muscle bands and atria are ignored, and the air capillaries are assumed to radiate outward directly from the parabronchial lumen.

The function of the model reflects the function of a real parabronchus. Venous blood, with a high concentration of CO_2 and a low concentration of O_2 , departs from a large vessel through a series of blood capillaries. The venous blood enters all blood capillaries with identical composition. As each blood capillary runs alongside its corresponding air capillary, CO_2 diffuses from the blood capillary into the air capillary and O_2 diffuses from the air capillary into the blood capillary. After undergoing gas exchange, the blood from all blood capillaries flows into a large vessel and mixes there to form arterial blood. Within the air capillary there is no flow of gas; mass transport occurs by diffusion. The diffusion of gases occurs so that the O_2 supply is constantly replenished from the parabronchial air and CO_2 constantly drains into the parabronchial air. Therefore, as gas flows down the parabronchial tube it loses O_2 and picks up CO_2 .

Explicitly, the more important assumptions of the model are:

1. All parabronchi composing the lung are structurally and functionally identical.
2. The model operates in steady state. Transient changes in ventilation, such as those occurring during the respiratory cycle, cannot be handled. Nor can transient changes in the partial pressure of gas or blood entering the lung be handled.

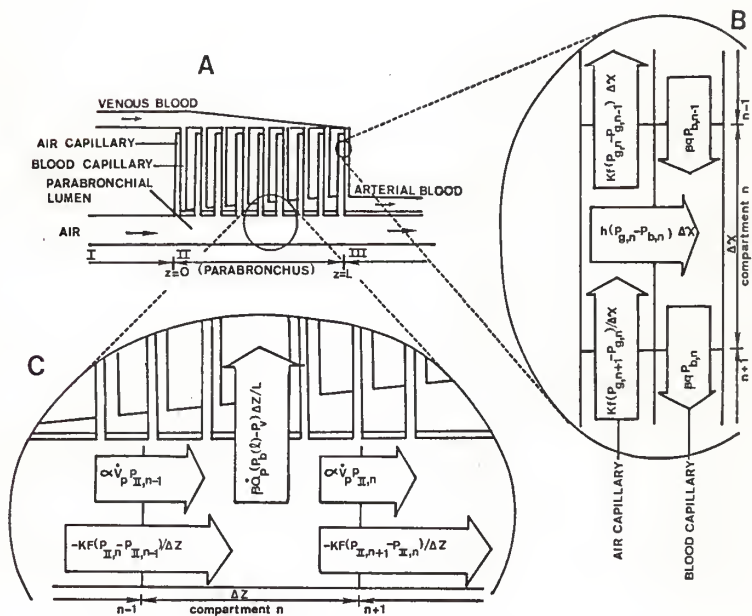


Figure 1. A: The parabronchial model, modified after Zeuthen. B: Detail of air capillary and blood capillary compartments. Expressions describing transport of the considered gas between compartments are shown. C: Detail of parabronchial luminal compartments. Expressions are shown which describe transport between luminal compartments by both bulk flow and diffusion and transport between a luminal compartment and the air capillaries which open into it.

3. The entire length of the parabronchus is equally perfused with blood.
4. The gas exchange surface is homogeneous. That is, it has equal diffusion capacity per unit area everywhere.
5. The physical structure of the atria and bands of smooth muscle is ignored.
6. No blood is shunted past the lungs without exposure to gas exchange surfaces.
7. There is no interaction between gas components. The Bohr and Haldane effects are not accounted for.

The model developed in this thesis generalizes in several important ways upon the model developed by Scheid and Piiper [2]. In their model, Scheid and Piiper neglected the structure of the air and blood capillaries. Gas exchange is represented as taking place between a thin sheet of blood flowing across the surface of a tubular parabronchus and the gas flowing through that tube. The direction of blood flow is perpendicular to the direction of gas flow, giving rise to the description of their model as "cross-current". In the model developed in the following pages, the air and blood capillaries are retained as separate structures, and expressions are developed which describe the variation in partial pressure of a particular gas component along the length of both the blood capillaries and the air capillaries. Also, in the model of Scheid and Piiper gas is assumed to move through the parabronchus by bulk flow alone, without diffusion of any gas component in the axial direction; in the model developed here both bulk flow and diffusion are accounted for. A further generalization in the developed model lies in the handling of the non-linear oxygen dissociation

curve. In the model of Scheid and Piiper, the oxygen dissociation curve has been represented as linear in order that the differential equations may easily be integrated. However, it has been found here that by handling those equations in a slightly different way and representing the dissociation curve by a polynomial of second or third order, the integration may still be performed. Use of a polynomial allows a much more accurate representation of the dissociation curve over the physiological range.

III. DERIVATION OF DIFFERENTIAL EQUATIONS

3.1 The Air Capillary-Blood Capillary Pair

The diffusion occurring between an air capillary and a blood capillary is considered. Although a mixture of different gases is present, it will be assumed that they do not interact. Attention can therefore be focused on a single component of the mixture.

Both the air capillary and blood capillary are represented as a string of homogeneous cells with mass transfer occurring across cell surfaces. Figure 1B illustrates this geometry.

A blood capillary cell, numbered n , will undergo mass transfer with blood capillary cells $n-1$ and $n+1$, and with air capillary cell n . The rate at which the gas component under consideration diffuses into blood capillary cell n from air capillary cell n is

$$h\Delta x(P_{g,n} - P_{b,n}) \quad (3.1-1)$$

The rate at which this component is transferred due to flow from blood capillary cell n to blood capillary cell $n+1$ minus the rate at which the component is transferred from blood capillary cell $n-1$ to blood capillary cell n is

$$f(C_{b,n} - C_{b,n-1}) \quad (3.1-2)$$

Under steady state conditions (3.1-1) and (3.1-2) are equal:

$$f(C_{b,n} - C_{b,n-1}) = h(P_{g,n} - P_{b,n})\Delta x \quad (3.1-3)$$

Dividing both sides of (3.1-3) by Δx , then taking the limit as $\Delta x \rightarrow 0$ leads to

$$\frac{dC_b}{dx} + \frac{h}{f} P_b = \frac{h}{f} P_g \quad (3.1-4)$$

In Cases 1, 2, 3, and 4 the simplifying assumption is made that C_b and P_b are connected by a relationship of the form

$$C_b = \beta_o + \beta P_b, \quad (3.1-5)$$

where β_o and β are constants, independent of variations in either P_b or x . Equation (3.1-5) substituted into (3.1-4) yields the differential equation

$$\frac{dP_b}{dx} + \frac{h}{\beta f} P_b = \frac{h}{\beta f} P_g. \quad (3.1-6)$$

Since it is assumed that the state of venous blood entering the lung is known, the initial condition for (3.1-6) is

$$P_b(x=0) = P_{b,v}, \text{ or } C_b(x=0) = C_{b,v}. \quad (3.1-7)$$

An air capillary cell, numbered n , will undergo mass transfer with air capillary cells $n-1$ and $n+1$, and with blood capillary cell n . The rate at which the component diffuses into air capillary cell n from blood capillary cell n is

$$h\Delta x(P_{b,n} - P_{g,n}). \quad (3.1-8)$$

In the actual air capillary where concentration of any gas component is a continuously changing quantity, the rate at which a component diffuses across a point in the air capillary is

$$-a\eta \frac{dP_g}{dx}. \quad (3.1-9)$$

In the discrete cell model, the rate at which the component diffuses from cell n to cell $n+1$ is

$$-a\eta \frac{P_{g,n+1} - P_{g,n}}{\Delta x}. \quad (3.1-10)$$

The rate at which the component diffuses from cell n to cell $n-1$ is

$$-\alpha\eta \frac{P_{g,n-1} - P_{g,n}}{\Delta x} . \quad (3.1-11)$$

Under steady state conditions, (3.1-8) can be equated to the sum of (3.1-10) and (3.1-11). Upon rearranging this becomes

$$\frac{1}{\Delta x} \left(\frac{P_{g,n+1} - P_{g,n}}{\Delta x} - \frac{P_{g,n} - P_{g,n-1}}{\Delta x} \right) - \frac{h}{\alpha\eta} P_{g,n} = - \frac{h}{\alpha\eta} P_{b,n} . \quad (3.1-12)$$

Taking the limit $\Delta x \rightarrow 0$,

$$\frac{d^2 P_g}{dx^2} - \frac{h}{\alpha\eta} P_g = - \frac{h}{\alpha\eta} P_b . \quad (3.1-13)$$

For the problem of diffusion between an air capillary and a blood capillary, it is assumed that the state of the gas at the air capillary opening is known. It is also assumed that the concentration gradient at the closed end of the capillary is zero, since there is no diffusion across the closed end. Hence the boundary conditions for (3.1-13) are:

$$P_g(x=l) = P_{g,p} = P_p , \quad (3.1-14)$$

and
$$\frac{dP_g}{dx}(x=0) = 0 . \quad (3.1-15)$$

A single compartment composed of a segment of an air capillary--blood capillary pair, as shown in Figure 2, is considered.

The rate at which the gas component enters the compartment at the upstream point is

$$\beta f P_{b,u} - \alpha\eta \frac{dP_{g,u}}{dx} . \quad (3.1-16)$$

The rate at which the gas component leaves the compartment at the downstream point is

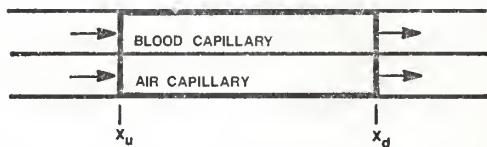


Figure 2. Single compartment composed of a segment of a blood-air capillary pair. The upstream and downstream ends of the compartment are at x_u and x_d , respectively.

$$\beta f P_{b,d} - \alpha \eta \frac{dP_{g,d}}{dx} . \quad (3.1-17)$$

Under steady state conditions (3.1-16) equals (3.1-17):

$$\beta f (P_{b,d} - P_{b,u}) = \alpha \eta \left(\frac{dP_{g,d}}{dx} - \frac{dP_{g,u}}{dx} \right) . \quad (3.1-18)$$

Now letting the upstream point be at $x=0$, and the downstream point be at $x=1$ causes (3.1-18) to become

$$\beta f (P_{b,a} - P_{b,v}) = \alpha \eta \frac{dP_{g,p}}{dx} , \quad (3.1-19)$$

where the boundary condition (3.1-15) has been used. Thus, the rate at which a single air capillary leaks the gas component into the parabronchus can be expressed either as

$$\beta f (P_{b,v} - P_{b,a}) , \quad (3.1-20)$$

or as

$$-\alpha \eta \frac{dP_{g,p}}{dx} . \quad (3.1-21)$$

3.2 The Parabronchus

As gas flows through the parabronchus the concentration of the gas component changes due to mass transfer between the parabronchus and the air capillaries. The model geometry to illustrate this process is shown in Figure 1C.

By a compartmentalization similar to that used on the capillaries, the parabronchus is considered to be divided into a string of cells which are numbered: $\dots, n-1, n, n+1, \dots$. They are all to have thickness Δz .

The rate at which the gas component is transferred due to flow from parabronchial cell n to cell $n+1$ minus the rate at which the component is transferred due to flow from cell $n-1$ to cell n is

$$F(C_{p,n} - C_{p,n-1}) . \quad (3.2-1)$$

This can be rewritten as

$$BF(P_{p,n} - P_{p,n-1}) . \quad (3.2-2)$$

The rate at which the component diffuses from parabronchial cell n to cell $n+1$ plus the rate at which it diffuses from cell n to cell $n-1$ is

$$-\phi\theta \frac{P_{p,n+1} - P_{p,n}}{\Delta x} + \phi\theta \frac{P_{p,n} - P_{p,n-1}}{\Delta x} . \quad (3.2-3)$$

The rate at which the gas component is transferred to the parabronchial cell from the air capillaries is found either from (3.1-20) to be

$$w\beta f(P_{b,v} - P_{b,a})\Delta z , \quad (3.2-4)$$

or from (3.1-21) to be

$$w\alpha\eta \frac{dP_{g,p}}{dx} \Delta z . \quad (3.2-5)$$

Under steady state conditions (3.2-4) can be equated to the sum of (3.2-2) and (3.2-3). Then dividing by Δz yields

$$-\frac{\phi\theta}{\Delta z} \left(\frac{P_{p,n+1} - P_{p,n}}{\Delta z} - \frac{P_{p,n} - P_{p,n-1}}{\Delta z} \right) + BF \left(\frac{P_{p,n} - P_{p,n-1}}{\Delta z} \right) = w\beta f(P_{b,v} - P_{b,a}) . \quad (3.2-6)$$

Taking the limit $\Delta z \rightarrow 0$ yields the differential equation

$$\theta \frac{d^2 P}{dz^2} - \frac{BF}{\phi} \frac{dP}{dz} = \frac{w\beta f}{\phi} (P_{b,a} - P_{b,v}) . \quad (3.2-7)$$

Similarly, equating (3.2-5) to the sum of (3.2-2) and (3.2-3) leads to the differential equation

$$\theta \frac{d^2 P}{dz^2} - \frac{BF}{\phi} \frac{dP}{dz} = -\frac{w\alpha\eta}{\phi} \frac{dP_{g,p}}{dx} . \quad (3.2-8)$$

The boundary conditions on (3.2-7) and (3.2-8) are

$$P_p(z=0) = P_{p,i} \quad (3.2-9)$$

and

$$\frac{dP_p(z=\lambda)}{dz} = 0 \quad (3.2-10)$$

A single compartment defined by the region between two cross-sectional cuts through the parabronchus perpendicular to its axis is considered. The compartment will contain the parabronchial lumen together with segments of the venous and arterial blood vessels as shown in Figure 3. The rate at which the gas component enters the parabronchial lumen at the upstream location is

$$FBP_{p,u} = \theta \phi \frac{dP_{p,u}}{dz} \quad (3.2-11)$$

The rate at which it leaves the parabronchial lumen at the downstream location is

$$FBP_{p,d} = \theta \phi \frac{dP_{p,d}}{dz} \quad (3.2-12)$$

The rate at which the dissolved gas component enters the compartment by way of arterial and venous vessels is

$$\beta(\dot{Q}_{v,d} P_{b,v} + \dot{Q}_{a,d} P_{b,a,d}) \quad (3.2-13)$$

The rate at which the dissolved gas component leaves the compartment by way of blood vessels is

$$\beta(\dot{Q}_{v,u} P_{b,v} + \dot{Q}_{a,u} P_{b,a,u}) \quad (3.2-14)$$

Under steady state conditions the quantity of gas entering the compartment equals the quantity of gas leaving the compartment, which leads to

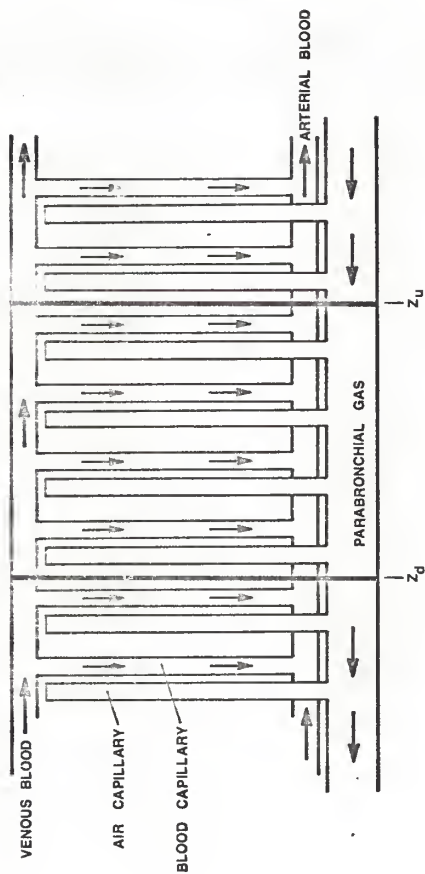


Figure 3. Single compartment defined by two cross-sectional cuts through the parabronchus. The upstream and downstream ends of the compartment are at z_u and z_d , respectively.

$$\begin{aligned}
 \text{FBP}_{p,u} - \theta\phi \frac{dP}{dz} \frac{P_{,u}}{P_{,d}} + \beta(\dot{Q}_{v,d} P_{b,v} + \dot{Q}_{a,d} P_{b,a,d}) \\
 = \text{FBP}_{p,d} - \theta\phi \frac{dP}{dz} \frac{P_{,d}}{P_{,u}} + \beta(\dot{Q}_{v,u} P_{b,v} + \dot{Q}_{a,v} P_{b,a,u}) .
 \end{aligned}
 \tag{3.2-15}$$

Taking $z_u=0$ and $z_d=\lambda$ yields

$$P_{p,u} = P_{p,i} ,$$

$$P_{p,d} = P_{p,e} ,$$

$$\frac{dP}{dz} \frac{P_{,u}}{P_{,d}} = \frac{dP}{dz} \frac{P_{,i}}{P_{,e}} ,$$

$$\frac{dP}{dz} \frac{P_{,d}}{P_{,u}} = 0 ,$$

$$\dot{Q}_{a,d} = \dot{Q}_{v,u} = 0 ,$$

$$\dot{Q}_{a,u} = \dot{Q}_{v,d} = \dot{Q} ,$$

$$P_{b,a,u} = \bar{P}_{b,a} .$$

Substitution of these boundary conditions into (3.2-15) and rearrangement yields the following expression for $\bar{P}_{b,a}$

$$\bar{P}_{b,a} = \frac{\text{FB}}{\beta\dot{Q}} (P_{p,i} - P_{p,e}) - \frac{\theta\phi}{\beta\dot{Q}} \frac{dP}{dz} \frac{P_{,i}}{P_{,e}} + P_{b,v} .
 \tag{3.2-16}$$

For convenient reference the differential equations and boundary conditions are listed in Table 3-1.

Table 3-1

$$\frac{dC_b}{dx} + \frac{h}{f} P_b = \frac{h}{f} P_g \quad (3.1-4)$$

$$\frac{dP_b}{dx} + \frac{h}{\beta f} P_b = \frac{h}{\beta f} P_g \quad (3.1-6)$$

$$C_b(x=0) = C_{b,v} \quad (3.1-7)$$

$$P_b(x=0) = P_{b,v} \quad (3.1-7)$$

$$\frac{d^2 P_g}{dx^2} - \frac{h}{\alpha \eta} P_g = - \frac{h}{\alpha \eta} P_b \quad (3.1-13)$$

$$P_g(x=l) = P_{g,p} = P_p \quad (3.1-14)$$

$$\frac{dP_g(x=0)}{dx} = 0 \quad (3.1-15)$$

$$\theta \frac{d^2 P}{dz^2} - \frac{\beta F}{\phi} \frac{dP}{dz} = \frac{w \beta f}{\phi} (P_{b,a} - P_{b,v}) \quad (3.2-7)$$

$$\theta \frac{d^2 P}{dz^2} - \frac{\beta F}{\phi} \frac{dP}{dz} = \frac{w \alpha \eta}{\phi} \frac{dP_{g,p}}{dx} \quad (3.2-8)$$

$$P_p(z=0) = P_{p,i} \quad (3.2-9)$$

$$\frac{dP_p(z=l)}{dz} = 0 \quad (3.2-10)$$

$$\bar{P}_{b,a} = P_{b,v} + \frac{FB}{\beta \dot{Q}} (P_{p,i} - P_{p,e}) - \frac{\theta \phi}{\beta \dot{Q}} \frac{dP_{p,i}}{dz} \quad (3.2-16)$$

IV. SOLUTION OF DIFFERENTIAL EQUATIONS

The model presented here consists of solutions to the set of equations appearing in Table 3-1. Five particular cases of the model are considered. In the Cases 1, 2, 3, and 4 it is assumed that C_b and P_b are connected by a relationship of the form

$$C_b = \beta_0 + \beta P_b$$

where β_0 and β are constants independent of variations in either P_b or x . Only one gas component is treated.

The differences between these four cases lie in the values assigned to the diffusion constants. A diffusion constant equal to infinity implies that diffusion occurs so easily that no partial pressure gradient can be maintained; a diffusion constant equal to zero implies no diffusion; a finite, non-zero diffusion constant implies diffusion as it actually occurs. Diffusion is assumed to occur only in the gas phase; the diffusion constant of blood is taken equal to zero in all the models. Diffusion can occur from gas to blood or from blood to gas, but not within the blood itself. The diffusion constants of air capillary gas and parabronchial gas, η and θ respectively, are assumed different in the derivation of Case 4 to allow for the possible effect of turbulence in the parabronchial gas on the effective diffusion constant.

In Case 1: $\eta = \infty$; $\theta = 0$

In Case 2: $\eta = \infty$; θ is finite, non-zero

In Case 3: η is finite, non-zero; $\theta = 0$

In case 4: η is finite, non-zero; θ is finite, non-zero

It can be shown that the Case 1 treated here is equivalent to the model of Scheid and Piiper [2].

4.1 Case 1 $\eta = \infty$; $\theta = 0$

The differential equation describing partial pressure of the gas component in the air capillary is (3.1-13) subject to the boundary conditions (3.1-14) and (3.1-15). Letting $\eta \rightarrow \infty$ causes (3.1-13) to take the form

$$\frac{d^2 P_g}{dx^2} = 0 \quad . \quad (4.1-1)$$

This implies

$$\frac{dP_g}{dx} = \text{constant} \quad . \quad (4.1-2)$$

Equations (4.1-2) and (3.1-15) imply

$$\frac{dP_g}{dx} = 0 \quad . \quad (4.1-3)$$

This implies that P_g , as a function of x , is a constant. Equation (3.1-14) then implies that along the entire length of the air capillary the partial pressure equals that of the parabronchial air the capillary opens into. Thus,

$$P_g = P_{g,p} = P_p \quad . \quad (4.1-4)$$

The differential equation describing partial pressure in the blood capillary is (3.1-6) subject to the boundary conditions (3.1-7) and to (4.1-4). The solution is

$$P_b = P_{b,v} \exp\left(\frac{-hx}{\beta f}\right) + P_p \left(1 - \exp\left(\frac{-hx}{\beta f}\right)\right) \quad . \quad (4.1-5)$$

Equation (4.1-5) gives the partial pressure of the gas component in the blood capillary as a function of location along that capillary.

The differential equation describing partial pressure of the gas in the parabronchus is (3.2-7) subject to the boundary conditions (3.2-9) and (3.2-10). Setting $\theta = 0$ causes (3.2-7) to take the form

$$\frac{dP}{dz} = \frac{w\beta f}{BF} (P_{b,v} - P_{b,a}) \quad (4.1-6)$$

To obtain the right side of (4.1-6), x is set equal to one in (4.1-5). This leads to

$$(P_{b,v} - P_{b,a}) + (P_{b,v} - P_p)(1 - \exp(\frac{-h\lambda}{\beta f})) \quad (4.1-7)$$

Equation (4.1-7) substituted into (4.1-6) yields

$$\frac{dP}{dz} = \frac{w\beta f}{BF} (1 - \exp(\frac{-h\lambda}{\beta f}))(P_{b,v} - P_p) \quad (4.1-8)$$

A constant, H , is defined as

$$H = w\beta f(1 - \exp(\frac{-h\lambda}{\beta f})) \quad (4.1-9)$$

Equation (4.1-8) becomes

$$\frac{dP}{dz} + \frac{H}{BF} P_p = \frac{H}{BF} P_{b,v} \quad (4.1-10)$$

The solution of (4.1-10) subject to (3.2-9) is

$$P_p = P_{p,i} \exp(\frac{-HZ}{BF}) + P_{b,v}(1 - \exp(\frac{-HZ}{BF})) \quad (4.1-11)$$

Equation (4.1-11) gives the partial pressure of the gas in the parabronchus as a function of location along the parabronchus. The partial pressure of the gas component in the arterial blood leaving the parabronchus is obtained from (3.2-16), recognizing that $\theta=0$ in that expression. The quantity $P_{p,e}$ required in (3.2-16) is found by replacing z with λ in (4.1-11). These substitutions yield

$$\bar{P}_{b,a} = P_{b,v}[1 - \frac{BF}{\beta Q} (1 - \exp(\frac{-H\lambda}{BF}))] + P_{p,i} \frac{BF}{\beta Q} (1 - \exp(\frac{-H\lambda}{BF})) \quad (4.1-12)$$

The form of (4.1-10) is important. It implies that the manner in which a substance diffuses from the venous blood through the intervening blood capillary-air capillary structure into the parabronchial gas is equivalent to the manner in which the substance would diffuse from a homogeneous compartment of venous blood across a simple interface into the parabronchial gas if the interface were characterized by a diffusing capacity, H . Conceptually, the blood capillary-air capillary exchange structure can be replaced by an equivalent interface between venous blood and parabronchial air compartments. This replacement is valid only insofar as the assumptions of Case 1 are valid.

4.2 Case 2 $\eta = \infty$; θ is finite, non-zero

In Case 2, as in Case 1, $\eta = \infty$. Hence the same solutions are obtained for P_g and P_b along the paired capillaries. They are

$$P_g = P_{b,p} = P_p, \quad (4.2-1)$$

$$\text{and} \quad P_b = P_{b,v} \exp\left(\frac{-hx}{\beta f}\right) + P_p \left(1 - \exp\left(\frac{-hx}{\beta f}\right)\right). \quad (4.2-2)$$

Also,

$$P_{b,v} - P_{b,a} = (P_{b,v} - P_p) \left(1 - \exp\left(\frac{-hx}{\beta f}\right)\right). \quad (4.2-3)$$

The differential equation describing partial pressure of the gas component in the parabronchus is (3.2-7) subject to the boundary conditions (3.2-9) and (3.2-10). Substituting (4.2-3) into (3.2-7) yields

$$\frac{d^2 P}{dz^2} - \frac{BF}{\theta \phi} \frac{dP}{dz} - \frac{H}{\theta \phi} P_p = -\frac{H}{\theta \phi} P_{b,v}. \quad (4.2-4)$$

where H is defined by (4.1-9). ψ and τ are defined as

$$\psi = \frac{H}{\theta \phi}, \quad \text{and} \quad \tau = \frac{BF}{\theta \phi}. \quad (4.2-5)$$

Now the differential equation appears as

$$\frac{d^2 P}{dz^2} - \tau \frac{dP}{dz} - \psi P = -\psi P_{bv} \quad (4.2-6)$$

An assumed solution of the homogeneous equation is

$$P = e^{sz} \quad (4.2-7)$$

Substitution into the homogeneous equation yields

$$s^2 - \tau s - \psi = 0 \quad (4.2-8)$$

which has the roots

$$s_1 = \frac{1}{2} (\tau + \sqrt{\tau^2 + 4\psi}) \quad (4.2-9)$$

and

$$s_2 = \frac{1}{2} (\tau - \sqrt{\tau^2 + 4\psi}) \quad (4.2-10)$$

The solution to (4.2-6) is of the form

$$P = b_1 e^{s_1 z} + b_2 e^{s_2 z} + P_{bv} \quad (4.2-11)$$

where b_1 and b_2 are to be determined.

The boundary condition (3.2-9) applied to (4.2-11) yields

$$P_{p,i} = b_1 + b_2 + P_{bv} \quad (4.2-12)$$

The boundary condition (3.2-10) applied to (4.2-11) yields

$$0 = b_1 s_1 e^{s_1 \lambda} + b_2 s_2 e^{s_2 \lambda} \quad (4.2-13)$$

Equations (4.2-12) and (4.2-13) can be solved for b_1 and b_2 , yielding

$$b_1 = \frac{s_2 e^{s_2 \lambda}}{s_2 e^{s_2 \lambda} - s_1 e^{s_1 \lambda}} (P_{p,i} - P_{bv}) \quad (4.2-14)$$

and

$$b_2 = \frac{-s_1 e^{s_1 \lambda}}{s_2 e^{s_2 \lambda} - s_1 e^{s_1 \lambda}} (P_{p,i} - P_{bv}) \quad (4.2-15)$$

Substitution of (4.2-14) and (4.2-15) into (4.2-11) yields the solution

$$P_p = P_{bv} + (P_{p,i} - P_{bv}) \frac{s_2 e^{s_2 \lambda} s_1 z - s_1 e^{s_1 \lambda} s_2 z}{s_2 e^{s_2 \lambda} - s_1 e^{s_1 \lambda}} \quad (4.2-16)$$

The derivative with respect to z is

$$\frac{dP}{dz} = (P_{p,i} - P_{bv}) \frac{s_1 s_2 (e^{s_2 \lambda} s_1 z - e^{s_1 \lambda} s_2 z)}{s_2 e^{s_2 \lambda} - s_1 e^{s_1 \lambda}} \quad (4.2-17)$$

The partial pressure of the dissolved gas component in the arterial blood is obtained from (3.2-16). The $P_{p,e}$ appearing in (3.2-16) is obtained by letting $z=\lambda$ in (4.2-16). The $dP_{p,i}/dz$ appearing in (3.2-16) is obtained by letting $z=0$ in (4.2-17).

$$\begin{aligned} \bar{P}_{b,a} = P_{bv} + (P_{p,i} - P_{bv}) \left\{ \frac{FB}{\beta Q} \left[1 - \frac{(s_2 - s_1) e^{s_1 \lambda} e^{s_2 \lambda}}{s_2 e^{s_2 \lambda} - s_1 e^{s_1 \lambda}} \right] \right. \\ \left. + \frac{\theta \phi}{\beta Q} \left[\frac{s_1 s_2 (e^{s_2 \lambda} s_1 - e^{s_1 \lambda} s_2)}{s_2 e^{s_2 \lambda} - s_1 e^{s_1 \lambda}} \right] \right\} \quad (4.2-18) \end{aligned}$$

In the development of Case 2 given above it is assumed that the partial pressure at the entrance to the parabronchus ($z=0$) is known. In an actual experimental situation, the partial pressure at exactly the entrance point may not be measurable; the partial pressure which might be measurable is that of the gas some distance upstream from the entrance. This upstream

gas could be tracheal gas or air sac gas in the real bird. Because of diffusion occurring between the gas in the parabronchial lumen and the gas which has not quite yet reached the parabronchus, the partial pressure of a gas component at the parabronchial entrance will not be the same as its partial pressure upstream. This effect will be greater at slower gas flow rates.

The geometrical relationships among preparabronchial, parabronchial, and postparabronchial gases are taken to be represented as shown in Figure 4. Qualitatively, the manner in which the partial pressure of a single gas component (CO_2) changes is also shown. Although Figure 4 does not accurately represent the geometrical relation between secondary bronchi and parabronchi, it should provide some insight into the diffusion processes occurring in the neighborhood of the parabronchial entrance.

Let P_I , P_{II} , and P_{III} denote the partial pressures in the three regions, respectively. The boundary conditions of this problem are:

$$\text{at } z \rightarrow \infty: P_I = P_{p,i} \quad , \quad \text{and} \quad \frac{d}{dz} P_I = 0 \quad . \quad (4.2-19)$$

$$\text{at } z=0: P_I = P_{II} \quad , \quad \text{and} \quad \frac{d}{dz} P_I = \frac{d}{dz} P_{II} \quad . \quad (4.2-20)$$

$$\text{at } z=\lambda: \frac{d}{dz} P_{II} = 0 \quad . \quad (4.2-21)$$

$$\text{at } z>\lambda: \frac{d}{dz} P_{III} = 0 \quad . \quad (4.2-22)$$

The differential equation for region I is found by setting $w_1 = 0$ in (3.2-8), which yields

$$\frac{d^2 P_I}{dz^2} - \tau \frac{dP_I}{dz} = 0 \quad , \quad (4.2-23)$$

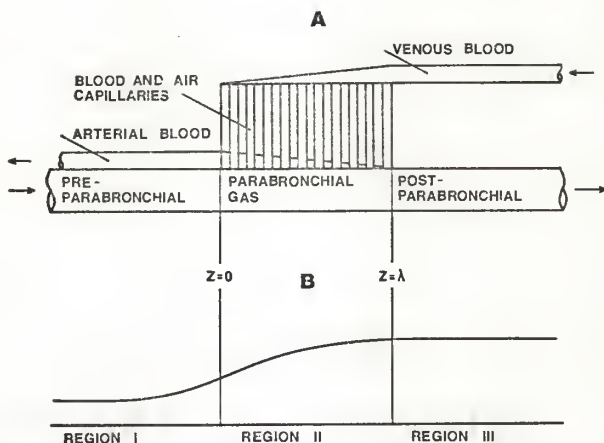


Figure 4. A: Geometrical relationship of pre-parabronchial, parabronchial, and post-parabronchial regions. B: Qualitative nature of CO_2 partial pressure along the parabronchus.

where again

$$\tau = \frac{BF}{\theta\phi} . \quad (4.2-24)$$

A solution,

$$P_I = e^{sz} , \quad (4.2-25)$$

is assumed. Substitution into (4.2-23) yields

$$s(s-\tau) = 0 , \quad (4.2-26)$$

which has the roots

$$s=0 , \quad \text{and} \quad s=\tau . \quad (4.2-27)$$

The solution to (4.2-23) is

$$P_I = b_3 e^{\tau z} + b_4 . \quad (4.2-28)$$

Condition (4.2-19) allows b_4 to be determined. Then,

$$P_I = b_3 e^{\tau z} + P_{p,i} . \quad (4.2-29)$$

The general expression for partial pressure of parabronchial gas in region II which has already been found is given by (4.2-11):

$$P_{II} = b_1 e^{s_1 z} + b_2 e^{s_2 z} + P_{b,v} . \quad (4.2-30)$$

Next b_1 , b_2 , and b_3 , must be found. From (4.2-29) and (4.2-30) and the boundary conditions (4.2-20) and (4.2-21), the following are determined:

$$b_3 + P_{p,i} = b_1 + b_2 + P_{b,v} , \quad (4.2-31)$$

$$b_3 \tau = b_1 s_1 + b_2 s_2 , \quad (4.2-32)$$

$$\text{and} \quad 0 = b_1 s_1 e^{s_1 \lambda} + b_2 s_2 e^{s_2 \lambda} . \quad (4.2-33)$$

The three equations can be solved for the b 's:

$$b_1 = \frac{\tau s_2 e^{s_2 \lambda} (P_{p,i} - P_{b,v})}{s_1 s_2 (e^{s_1 \lambda} - e^{s_2 \lambda}) + \tau (s_2 e^{s_2 \lambda} - s_1 e^{s_1 \lambda})} , \quad (4.2-34)$$

$$b_2 = \frac{-\tau s_1 e^{s_1 \lambda} (P_{p,i} - P_{bv})}{s_1 s_2 (e^{s_1 \lambda} - e^{s_2 \lambda}) + \tau (s_2 e^{s_2 \lambda} - s_1 e^{s_1 \lambda})}, \quad (4.2-35)$$

and

$$b_3 = \frac{s_1 s_2 (e^{s_2 \lambda} - e^{s_1 \lambda}) (P_{p,i} - P_{bv})}{s_1 s_2 (e^{s_1 \lambda} - e^{s_2 \lambda}) + \tau (s_2 e^{s_2 \lambda} - s_1 e^{s_1 \lambda})}. \quad (4.2-36)$$

Substitution of (4.2-34), (4.2-35), and (4.2-36) into (4.2-29) and (4.2-30) yields

$$P_I = P_{p,i} + (P_{p,i} - P_{bv}) \frac{s_1 s_2 e^{\tau z} (e^{s_1 \lambda} - e^{s_2 \lambda})}{s_1 s_2 (e^{s_1 \lambda} - e^{s_2 \lambda}) + \tau (s_2 e^{s_2 \lambda} - s_1 e^{s_1 \lambda})}, \quad (4.2-37)$$

and

$$P_{II} = P_{bv} + (P_{p,i} - P_{bv}) \frac{\tau s_2 e^{s_1 z} e^{s_2 \lambda} - \tau s_1 e^{s_2 z} e^{s_1 \lambda}}{s_1 s_2 (e^{s_1 \lambda} - e^{s_2 \lambda}) + \tau (s_2 e^{s_2 \lambda} - s_1 e^{s_1 \lambda})}. \quad (4.2-38)$$

To find the partial pressure in the arterial blood, substitute into 3.2-16. $P_{p,e}$ is given by (4.2-38) with $z=\lambda$; the derivative $dP_{p,i}/dz$ is taken equal to zero, since for z much less than zero the slope of the partial pressure curve approaches zero.

$$P_{b,a} = P_{bv} + (P_{p,i} - P_{bv}) \frac{FB}{\dot{Q}} \left[1 - \frac{\tau e^{s_1 \lambda} e^{s_2 \lambda} (s_2 - s_1)}{s_1 s_2 (e^{s_1 \lambda} - e^{s_2 \lambda}) + \tau (s_2 e^{s_2 \lambda} - s_1 e^{s_1 \lambda})} \right]. \quad (4.2-39)$$

Equations (4.2-37) and (4.2-38) give the partial pressure along the parabronchus and (4.2-39) gives the partial pressure in arterial blood when the boundary conditions specify the partial pressure of gas at a location far upstream ($z \rightarrow \infty$).

4.3 Case 3 η is finite, non-zero; $\theta=0$

In case 3 diffusion within the air capillary is taken into account. The differential equation describing the partial pressures P_g and P_b along the paired capillaries are (3.1-6) and (3.1-13), subject to the boundary conditions (3.1-7), (3.1-14) and (3.1-15).

Figure 5 is a simulation diagram of (3.1-6) and (3.1-13).

The state variables are selected as

$$y_1 = P_g, \quad y_2 = \frac{dP_g}{dx}, \quad \text{and} \quad y_3 = P_b. \quad (4.3-1)$$

Quantities σ and ρ are defined as

$$\sigma = \frac{h}{\eta}, \quad \text{and} \quad \rho = \frac{h}{\beta f}. \quad (4.3-2)$$

The state variable equation is

$$\frac{d}{dx} \begin{bmatrix} y_1 \\ y_2 \\ y_3 \end{bmatrix} = \begin{bmatrix} 0 & 1 & 0 \\ \sigma & 0 & -\sigma \\ \rho & 0 & -\rho \end{bmatrix} \begin{bmatrix} y_1 \\ y_2 \\ y_3 \end{bmatrix}. \quad (4.3-3)$$

Taking the Laplace transform of (4.3-3) and rearranging yields

$$\begin{bmatrix} s & -1 & 0 \\ -\sigma & s & \sigma \\ -\rho & 0 & s+\rho \end{bmatrix} \begin{bmatrix} Y_1 \\ Y_2 \\ Y_3 \end{bmatrix} = \begin{bmatrix} y_{10} \\ y_{20} \\ y_{30} \end{bmatrix}, \quad (4.3-4)$$

where s is the transform variable; the Y 's are Laplace transforms of the y 's; and the subscript 0 on the y 's signifies their initial values at $x=0$.

Multiplying both sides of (4.3-4) by the inverse of the matrix appearing there yields

$$\begin{bmatrix} Y_1 \\ Y_2 \\ Y_3 \end{bmatrix} = \frac{1}{s(s-s_1)(s-s_2)} \begin{bmatrix} s(s+\rho) & (s+\rho) & -\sigma \\ s\sigma & s(s+\rho) & -s\sigma \\ s\rho & \rho & s^2 - \sigma^2 \end{bmatrix} \begin{bmatrix} Y_{10} \\ Y_{20} \\ Y_{30} \end{bmatrix}, \quad (4.3-5)$$

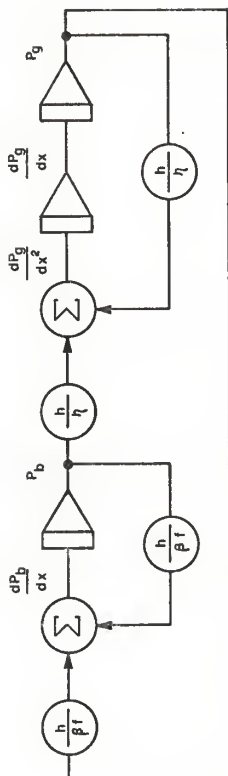


Figure 5. Simulation diagram of equations (3.1-6) and (3.1-13)

where

$$s_1 = \frac{-\rho}{2} + \frac{\sqrt{\rho^2 + 4\sigma}}{2}, \text{ and } s_2 = \frac{-\rho}{2} - \frac{\sqrt{\rho^2 + 4\sigma}}{2}. \quad (4.3-6)$$

The technique of expansion in partial fractions, when applied to (4.3-5), yields

$$\begin{bmatrix} y_1 \\ y_2 \\ y_3 \end{bmatrix} = \left[\frac{M_1}{s} + \frac{M_2}{s-s_1} + \frac{M_3}{s-s_2} \right] \begin{bmatrix} y_{10} \\ y_{20} \\ y_{30} \end{bmatrix}, \quad (4.3-7)$$

where

$$M_1 = \frac{1}{s_1 s_2} \begin{bmatrix} 0 & \rho & -\sigma \\ 0 & 0 & 0 \\ 0 & \rho & -\sigma \end{bmatrix}, \quad (4.3-8)$$

$$M_2 = \frac{1}{s_1(s_1-s_2)} \begin{bmatrix} s_1(s_1+\rho) & s_1+\rho & -\sigma \\ s_1\sigma & s_1(s_1+\rho) & -s_1\sigma \\ s_1\rho & \rho & s_1^2-\sigma \end{bmatrix}, \quad (4.3-9)$$

and

$$M_3 = \frac{1}{s_2(s_2-s_1)} \begin{bmatrix} s_2(s_2+\rho) & s_2+\rho & -\sigma \\ s_2\sigma & s_2(s_2+\rho) & -s_2\sigma \\ s_2\rho & \rho & s_2^2-\sigma \end{bmatrix}. \quad (4.3-10)$$

The solution for the state variables is

$$\begin{bmatrix} y_1 \\ y_2 \\ y_3 \end{bmatrix} = \left[M_1 + M_2 e^{s_1 x} + M_3 e^{s_2 x} \right] \begin{bmatrix} y_{10} \\ y_{20} \\ y_{30} \end{bmatrix}, \quad (4.3-11)$$

which can be written as

$$\begin{bmatrix} y_1 \\ y_2 \\ y_3 \end{bmatrix} = \begin{bmatrix} m_{11} & m_{12} & m_{13} \\ m_{21} & m_{22} & m_{23} \\ m_{31} & m_{32} & m_{33} \end{bmatrix} \begin{bmatrix} y_{10} \\ y_{20} \\ y_{30} \end{bmatrix}, \quad (4.3-12)$$

where

$$m_{11} = \frac{(s_1 + \rho)}{(s_1 - s_2)} e^{s_1 x} + \frac{(s_2 + \rho)}{(s_2 - s_1)} e^{s_2 x}, \quad (4.3-13)$$

$$m_{12} = \frac{\rho}{s_1 s_2} + \frac{s_1 + \rho}{s_1 (s_1 - s_2)} e^{s_1 x} + \frac{s_2 + \rho}{s_2 (s_2 - s_1)} e^{s_2 x}, \quad (4.3-14)$$

$$m_{13} = \frac{-\sigma}{s_1 s_2} + \frac{-\sigma}{s_1 (s_1 - s_2)} e^{s_1 x} + \frac{-\sigma}{s_2 (s_2 - s_1)} e^{s_2 x}, \quad (4.3-15)$$

$$m_{21} = \frac{\sigma}{(s_1 - s_2)} e^{s_1 x} + \frac{\sigma}{(s_2 - s_1)} e^{s_2 x}, \quad (4.3-16)$$

$$m_{22} = \frac{(s_1 + \rho)}{(s_1 - s_2)} e^{s_1 x} + \frac{(s_2 + \rho)}{(s_2 - s_1)} e^{s_2 x}, \quad (4.3-17)$$

$$m_{23} = \frac{-\sigma}{(s_1 - s_2)} e^{s_1 x} + \frac{-\sigma}{(s_2 - s_1)} e^{s_2 x}, \quad (4.3-18)$$

$$m_{31} = \frac{\rho}{(s_1 - s_2)} e^{s_1 x} + \frac{\rho}{(s_2 - s_1)} e^{s_2 x}, \quad (4.3-19)$$

$$m_{32} = \frac{\rho}{s_1 s_2} + \frac{\rho}{s_1 (s_1 - s_2)} e^{s_1 x} + \frac{\rho}{s_2 (s_2 - s_1)} e^{s_2 x}, \quad (4.3-20)$$

$$\text{and} \quad m_{33} = \frac{-\sigma}{s_1 s_2} + \frac{s_1^2 - \sigma}{s_1 (s_1 - s_2)} e^{s_1 x} + \frac{s_2^2 - \sigma}{s_2 (s_2 - s_1)} e^{s_2 x}. \quad (4.3-21)$$

Equation (4.3-12) is not yet a usable solution. The boundary conditions, given by (3.1-7), (3.1-14), and (3.1-15), are constraints on different quantities than those which appear on the right side of (4.3-12). The solution must be given in terms of the values of y_2 and y_3 at $x=0$ and y_1 at $x=l$. Substituting $x=l$ into (4.3-12) and denoting by the subscript, l , the values taken at $x=l$, yields

$$\begin{bmatrix} y_{1l} \\ y_{2l} \\ y_{3l} \end{bmatrix} = \begin{bmatrix} m_{11l} & m_{12l} & m_{13l} \\ m_{21l} & m_{22l} & m_{23l} \\ m_{31l} & m_{32l} & m_{33l} \end{bmatrix} \begin{bmatrix} y_{10} \\ y_{20} \\ y_{30} \end{bmatrix} . \quad (4.3-22)$$

The known boundary values are y_{1l} , y_{20} , and y_{30} ; the unknown boundary values are y_{10} , y_{2l} , and y_{3l} . Solving for the unknowns in terms of the knowns yields

$$\begin{bmatrix} y_{10} \\ y_{2l} \\ y_{3l} \end{bmatrix} = \frac{-1}{m_{11l}} \begin{bmatrix} -1 & m_{12l} & m_{13l} \\ -m_{21l} & (m_{21l}m_{12l} - m_{11l}m_{22l}) & (m_{21l}m_{13l} - m_{11l}m_{23l}) \\ -m_{31l} & (m_{31l}m_{12l} - m_{11l}m_{32l}) & (m_{31l}m_{13l} - m_{11l}m_{33l}) \end{bmatrix} \begin{bmatrix} y_{1l} \\ y_{20} \\ y_{30} \end{bmatrix} . \quad (4.3-23)$$

The quantity y_{10} is

$$y_{10} = \frac{1}{m_{11l}} [y_{1l} - m_{12l}y_{20} - m_{13l}y_{30}] . \quad (4.3-24)$$

It follows from (4.3-24) that

$$\begin{bmatrix} y_{10} \\ y_{20} \\ y_{30} \end{bmatrix} = \frac{1}{m_{11l}} \begin{bmatrix} 1 & -m_{12l} & -m_{13l} \\ 0 & m_{11l} & 0 \\ 0 & 0 & m_{11l} \end{bmatrix} \begin{bmatrix} y_{1l} \\ y_{20} \\ y_{30} \end{bmatrix} . \quad (4.3-25)$$

Substituting (4.3-25) into (4.3-12) yields

$$\begin{bmatrix} y_1 \\ y_2 \\ y_3 \end{bmatrix} = \frac{1}{m_{11l}} \begin{bmatrix} m_{11} & (m_{12}m_{11l} - m_{11}m_{12l}) & (m_{13}m_{11l} - m_{11}m_{13l}) \\ m_{21} & (m_{22}m_{11l} - m_{21}m_{12l}) & (m_{23}m_{11l} - m_{21}m_{13l}) \\ m_{31} & (m_{32}m_{11l} - m_{31}m_{12l}) & (m_{33}m_{11l} - m_{31}m_{13l}) \end{bmatrix} \begin{bmatrix} y_{1l} \\ y_{20} \\ y_{30} \end{bmatrix} . \quad (4.3-26)$$

Equation (4.3-26) is the solution for y_1 , y_2 , and y_3 (that is P_g , $\frac{d}{dx} P_g$, and P_b) as a function of x along the paired capillaries when diffusion within the air capillary is taken into account, and it is given in terms of the known boundary conditions. It is equivalent to the following three equations:

$$P_g = \frac{m_{11}}{m_{11l}} P_p + \frac{(m_{13}m_{11l} - m_{11}m_{13l})}{m_{11l}} P_{b,v} , \quad (4.3-27)$$

$$\frac{dP_g}{dx} = \frac{m_{21}}{m_{11l}} P_p + \frac{(m_{23}m_{11l} - m_{21}m_{13l})}{m_{11l}} P_{h,v}, \quad (4.3-28)$$

$$\text{and} \quad P_b = \frac{m_{31}}{m_{11l}} P_p + \frac{(m_{33}m_{11l} - m_{31}m_{13l})}{m_{11l}} P_{h,v}. \quad (4.3-29)$$

The differential equation describing partial pressure in the parabronchus is (3.2-8) subject to the boundary conditions (3.2-9) and (3.2-10). The specialization $\theta=0$, which implies there is only bulk flow through the parabronchus, causes (3.2-8) to assume the form

$$\frac{dP_p}{dz} = \frac{-w\alpha\eta}{BF} \frac{dP_g}{dx}. \quad (4.3-30)$$

Substituting (4.3-28) into (4.3-30) and rearranging yields

$$\frac{dP_p}{dz} = \frac{-w\alpha\eta}{BF} \left(\frac{m_{21l}}{m_{11l}} \right) P_p + \left(\frac{m_{11l}m_{23l}}{m_{21l}} - m_{13l} \right) P_{bv}. \quad (4.3-31)$$

The quantities H and δ are defined as

$$H = w\alpha\eta \left(\frac{m_{21l}}{m_{11l}} \right), \quad (4.3-32)$$

$$\text{and} \quad \delta - 1 = \left(\frac{m_{11l}m_{23l}}{m_{21l}} - m_{13l} \right). \quad (4.3-33)$$

Then (4.3-31) assumes the form

$$\frac{dP_p}{dz} + \frac{H}{BF} P_p = \frac{H}{BF} (1-\delta) P_{b,v}. \quad (4.3-34)$$

Equation (4.3-34) has the solution

$$P_p = P_{p,i} \exp\left(\frac{-Hz}{BF}\right) + P_{b,v}(1-\delta) \left[1 - \exp\left(\frac{-Hz}{BF}\right) \right]. \quad (4.3-35)$$

Equation (4.3-35) gives the partial pressure of the gas component in the parabronchus as a function of location along the parabronchus when there is diffusion within the air capillaries and only bulk flow through the parabronchus. The observation made in connection with Case 1 that the blood

capillary-air capillary structure can be replaced by an equivalent simple interface between blood and gas compartments is precluded in Case 3 by the appearance of $\delta \neq 0$.

The partial pressure of the dissolved gas component in the arterial blood is obtained from (3.2-16), recognizing that $\theta=0$ and that $P_{p,e}$ is obtained by letting $z=\lambda$ in (4.3-35). The result is

$$\begin{aligned} \bar{P}_{b,a} = P_{b,v} & \left[1 - \frac{FB}{\beta Q} (1-\delta) (1 - \exp(\frac{-H\lambda}{BF})) \right] \\ & + P_{p,i} \left(\frac{FB}{\beta Q} \right) (1 - \exp(\frac{-H\lambda}{BF})) . \end{aligned} \quad (4.3-36)$$

4.4 Case 4: η is finite, non-zero; θ is finite, non-zero

In Case 4, as in Case 3, η is finite and non-zero. Hence the same solutions are obtained for P_g , P_b , and $\frac{dP}{dx}$ along the paired capillaries. They are

$$P_g = \frac{m_{11}}{m_{11l}} P_p + \frac{(m_{13}m_{11l} - m_{11}m_{13l})}{m_{11l}} P_{b,v} , \quad (4.4-1)$$

$$P_b = \frac{m_{31}}{m_{11l}} P_p + \frac{(m_{33}m_{11l} - m_{31}m_{13l})}{m_{11l}} P_{b,v} , \quad (4.4-2)$$

$$\text{and} \quad \frac{dP}{dx} = \frac{m_{21l}}{m_{11l}} P_p - \frac{(m_{21l}m_{13l} - m_{11l}m_{23l})}{m_{11l}} P_{b,v} . \quad (4.4-3)$$

The differential equation describing partial pressure in the parabronchus is (3.2-8) subject to the boundary conditions (3.2-9) and (3.2-10). Substituting (4.4-3) into (3.2-8) and rearranging yields

$$\begin{aligned} \frac{d^2 P}{dz^2} - \frac{BF}{\theta \phi} \frac{dP}{dz} - \left(\frac{w\alpha\eta}{\theta \phi} \frac{m_{21l}}{m_{11l}} \right) P_p = \frac{-w\alpha\eta}{\theta \phi} \frac{m_{21l}}{m_{11l}} \left[m_{13l} - \frac{m_{11l}m_{23l}}{m_{21l}} \right] P_{b,v} . \end{aligned} \quad (4.4-4)$$

The quantities τ_d , ψ_d , and δ_d are defined as

$$\tau_d = \frac{BF}{\theta\phi} \quad ; \quad \psi_d = \frac{wan}{\theta\phi} \frac{m_{21l}}{m_{11l}} \quad ; \quad \text{and} \quad 1 + \delta_d = m_{13l} - \frac{m_{11l}m_{23l}}{m_{21l}} \quad . \quad (4.4-5)$$

Now the differential equation appears as

$$\frac{d^2 P}{dz^2} - \tau_d \frac{dP}{dz} - \psi_d P = -\psi_d (1 + \delta_d) P_{bv} \quad . \quad (4.4-6)$$

By comparison of (4.4-6) with (4.2-6) it is apparent that the solutions for Case 4 are obtained from the Case 2 solutions by making the replacements

$$\begin{aligned} \tau &\rightarrow \tau_d \quad , \\ \psi &\rightarrow \psi_d \quad , \\ P_{bv} &\rightarrow (1 + \delta_d) P_{bv} \quad , \\ s_1 &\rightarrow s_{d1} \quad , \end{aligned} \quad (4.4-7)$$

and

$$s_2 \rightarrow s_{d2} \quad ,$$

where s_{d1} and s_{d2} are functions of ψ_d and τ_d . Assuming that $P_{p,i}$ at the parabronchial entrance is known and substituting into the case 2 solutions (4.2-16), (4.2-17), and (4.2-18) yields

$$P_p = (1 + \delta_d) P_{bv} + (P_{p,i} - (1 + \delta_d) P_{bv}) \frac{s_{d2}^{\lambda} e^{s_{d1} z} - s_{d1}^{\lambda} e^{s_{d2} z}}{s_{d2}^{\lambda} e^{s_{d2} z} - s_{d1}^{\lambda} e^{s_{d1} z}} \quad , \quad (4.4-8)$$

$$\frac{dP}{dz} = (P_{p,i} - (1 + \delta_d) P_{bv}) \frac{s_{d1} s_{d2} (e^{s_{d2} z} e^{s_{d1} z} - e^{s_{d1} z} e^{s_{d2} z})}{s_{d2}^{\lambda} e^{s_{d2} z} - s_{d1}^{\lambda} e^{s_{d1} z}} \quad , \quad (4.4-9)$$

and

$$P_{b,a} = (1+\delta_d)P_{bv} + (P_{p,i} - (1+\delta_d)P_{bv}) \left\{ \frac{FB}{\beta Q} \left[1 - \frac{(s_{d2}^{-s_{d1}}) e^{s_{d1}^\lambda} e^{s_{d2}^\lambda}}{s_{d2} e^{s_{d2}^\lambda} - s_{d1} e^{s_{d1}^\lambda}} \right] + \frac{\theta \phi}{\beta Q} \left[\frac{s_{d1} s_{d2} (e^{s_{d2}^\lambda} - e^{s_{d1}^\lambda})}{s_{d2} e^{s_{d2}^\lambda} - s_{d1} e^{s_{d1}^\lambda}} \right] \right\}. \quad (4.4-10)$$

When diffusion occurs within the air capillaries, diffusion and bulk flow occur within the parabronchus, and the state of the gas at $z=0$ is known, then (4.4-8) and (4.4-9) describe the partial pressure and its derivative along the parabronchus and (4.4-10) describes the partial pressure of arterial blood. Assuming that $P_{p,i}$ at a location far upstream is known and substituting into (4.2-37), (4.2-38), and (4.2-39) yields

$$P_I = P_{p,i} + (P_{p,i} - (1+\delta_d)P_{bv}) \frac{s_{d1} s_{d2} e^{\tau_d^2} (e^{s_{d1}^\lambda} - e^{s_{d2}^\lambda})}{s_{d1} s_{d2} (e^{s_{d1}^\lambda} - e^{s_{d2}^\lambda}) + \tau_d (s_{d2} e^{s_{d2}^\lambda} - s_{d1} e^{s_{d1}^\lambda})}, \quad (4.4-11)$$

$$P_{II} = (1+\delta_d)P_{bv} + (P_{p,i} - (1+\delta_d)P_{bv}) \frac{\tau_d s_{d2} e^{s_{d1} z} e^{s_{d2}^\lambda} - \tau_d s_{d1} e^{s_{d2} z} e^{s_{d1}^\lambda}}{s_{d1} s_{d2} (e^{s_{d1}^\lambda} - e^{s_{d2}^\lambda}) + \tau_d (s_{d2} e^{s_{d2}^\lambda} - s_{d1} e^{s_{d1}^\lambda})}, \quad (4.4-12)$$

and

$$P_{b,a} = (1+\delta_d)P_{bv} + (P_{p,i} - (1+\delta_d)P_{bv}) \frac{FB}{\beta Q} \left[1 - \frac{\tau_d e^{s_{d1}^\lambda} e^{s_{d2}^\lambda} (s_{d2} - s_{d1})}{s_{d1} s_{d2} (e^{s_{d1}^\lambda} - e^{s_{d2}^\lambda}) + \tau_d (s_{d2} e^{s_{d2}^\lambda} - s_{d1} e^{s_{d1}^\lambda})} \right]. \quad (4.4-13)$$

When diffusion occurs within the air capillaries, diffusion and bulk flow occur within the parabronchus, and the state of the gas at $z \rightarrow \infty$ is known, then (4.4-11) and (4.4-12) describe the partial pressure along the parabronchus and (4.4-13) describes the partial pressure of arterial blood.

In APPENDIX B an independent derivation is given for the solutions for partial pressure along the blood capillaries, air capillaries, and parabronchus when it is assumed that diffusion occurs within the air capillaries, both diffusion and bulk flow occur within the parabronchus, and the state of the gas at $z \rightarrow \infty$ is known.

4.5 Case 5

In Cases 1, 2, 3, and 4 it was assumed that the partial pressure, P , and concentration, C , of a gas component in blood were connected by a linear relationship of the form

$$C = k_1 + k_2 P ,$$

where k_1 and k_2 are constants

If the gas component of interest is oxygen the actual situation is more complicated than this. The oxygen dissociation curve, a curve of concentration vs. partial pressure, appears as shown in Figure 6.

Due to the effects named after Bohr and Haldane, there is an interaction between oxygen and carbon dioxide concentrations. A change in oxygen partial pressure will cause a shift of the carbon dioxide dissociation curve, and a change in carbon dioxide partial pressure will cause a distortion of the oxygen dissociation curve. In Case 5, as in the previous cases, interactions between oxygen and carbon dioxide are neglected and a single component, oxygen, is treated. This component is assumed to have the dissociation curve appearing in Figure 6, and the curve is not distorted

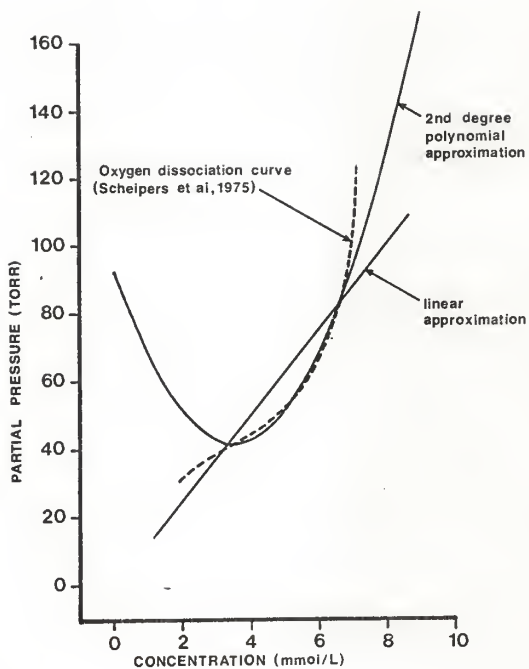


Figure 6. Oxygen dissociation curve, linear approximation to it, and 2nd degree polynomial approximation to it.

due to the Bohr or Haldane effects. The technique of case 5 has not been used for carbon dioxide since this gas has a dissociation curve that is very linear over the physiological range.

In Case 5 the same assumptions regarding the diffusion constant are made as in Case 1; that is $\theta \rightarrow \infty$ and $n=0$. It can be seen from the computed results of Figure 9A that this is a reasonable assumption if the ventilation rate is not too low. The same argument given in the discussion of Case 1 implies here also that P_g equals a constant along the length of an air capillary.

In Cases 1, 2, 3, and 4 the solution was found for partial pressure, P_b , along the blood capillary. By contrast, in Case 5 it is more convenient to solve for the concentration, C_b . The differential equation describing gas diffusion between an air capillary and a blood capillary is (3.1-4) subject to the boundary condition (3.1-7). Knowledge of the dissociation curve, as given in Figure 6, implies existence of a mathematical relationship giving P_b as a function of C_b . It is assumed here that such a function can be well represented as a polynomial of second degree over the C_b range of interest:

$$P_b = q_2 C_b^2 + q_1 C_b + q_0 \quad (4.5-1)$$

Substitution of (4.5-1) into (3.1-4), rearrangement and integration, yields

$$\int \frac{dC_b}{q_2 C_b^2 + q_1 C_b + (q_0 - P_g)} + \int \frac{h \, dx}{f} = 0 \quad (4.5-2)$$

The integral appearing in (4.5-2) is found in reference [6]. The lower limit is $C_b(x=0) = C_{bv}$. A term r_1 is defined as

$$r_1 = 4q_2(q_0 - P_g) - q_1^2 \quad (4.5-3)$$

There are two cases to consider.

If $r_1 > 0$

$$\frac{2}{\sqrt{r_1}} \tan^{-1} \frac{2q_2 C_b + q_1}{\sqrt{r_1}} \bigg|_{C_{bv}}^{C_b} + \frac{hx}{f} = 0, \quad (4.5-4)$$

Then

$$C_b = \frac{-q_1}{2q_2} + \frac{\sqrt{r_1}}{2q_2} \tan \left[\tan^{-1} \left(\frac{2q_2 C_{bv} + q_1}{\sqrt{r_1}} \right) - \frac{hx\sqrt{r_1}}{2f} \right]. \quad (4.5-5)$$

If $r_1 < 0$

$$\frac{1}{\sqrt{-r_1}} \log \frac{2q_2 C_b + q_1 - \sqrt{-r_1}}{2q_2 C_b + q_1 + \sqrt{-r_1}} \bigg|_{C_{bv}}^{C_b} + \frac{hx}{f} = 0, \quad (4.5-6)$$

Then

$$C_b = \frac{\sqrt{-r_1}(1 + r_2 \exp(-hx\sqrt{-r_1}/f)) - q_1(1 - r_2 \exp(-hx\sqrt{-r_1}/f))}{2q_2(1 - r_2 \exp(-hx\sqrt{-r_1}/f))}, \quad (4.5-7)$$

where

$$r_2 = \frac{2q_2 C_{bv} + q_1 - \sqrt{-r_1}}{2q_2 C_{bv} + q_1 + \sqrt{-r_1}}. \quad (4.5-8)$$

If a more accurate representation of the dissociation curve is desired, in the place of (4.5-1) a third order polynomial can be used. The integral which then appears in (4.5-2) can be found in integral tables (reference [6]).

Equation (4.5-5) or (4.5-7) gives the concentration of the gas component dissolved in blood if the state of incoming venous blood is known and if the state of the parabronchial gas into which the air capillary opens is known. Due to the form of these expressions, however, it has not been possible to proceed as was done with the Cases 1, 2, 3, and 4 and obtain an analytical solution for the partial pressure along the parabronchus. To obtain these parabronchial partial pressures, a discrete rather than continuous representation of the parabronchus has been used.

The parabronchus is considered to be divided into a string of cells which are numbered: ...n-1, n, n+1, ... They all have thickness, Δz , as shown in Figure 1C.

It is assumed that a value is given for the partial pressure of the gas component in cell n, P_{pn} . Then C_{bn} is computable from (4.5-5) or (4.5-7). Setting $x=1$ in the expression for C_{bn} yields C_{ban} . (The additional subscript n on C_b indicates that the capillary is located on cell n). From (3.1-2a), the rate at which the component is transferred from a single blood capillary into the parabronchus is

$$f(C_{bv} - C_{ban}) . \quad (4.5-9)$$

If this gas enters cell n, it will change the value P_{pn} which has already been assumed for that cell. So let it enter cell n+1. The total gas entering cell n+1 from the capillaries physically located on cell n is

$$fw(C_{bv} - C_{bsn})\Delta z . \quad (4.5-10)$$

The rate at which the component flows directly from cell n into cell n+1 is

$$FC_{pn} , \quad (4.5-11)$$

where

$$C_{pn} = BP_{pn} . \quad (4.5-12)$$

Under steady state conditions the sum of (4.5-10) and (4.5-11) equals the rate at which the component flows out of cell $n+1$. Thus,

$$fw(C_{bv} - C_{ban})\Delta z + FC_{pn} = FC_{p,n+1} . \quad (4.5-13)$$

It follows that

$$P_{p,n+1} = \frac{fw(C_{bv} - C_{ban})\Delta z + FC_{pn}}{BF} . \quad (4.5-14)$$

The process can now be repeated to calculate $P_{p,n+2}$. In this way the partial pressure in all the cells along the parabronchus can be calculated, given that the partial pressure in the first cell is P_{pi} .

The oxygen uptake affected by a single parabronchus can be expressed either as

$$\dot{Q}(\bar{C}_{ba} - C_{bv}) , \quad (4.5-15)$$

or as

$$FB(P_{pi} - P_{pe}) . \quad (4.5-16)$$

Equating (4.5-15) and (4.5-16) and solving for \bar{C}_{ba} yields

$$\bar{C}_{ba} = C_{bv} + \frac{FB}{\dot{Q}} (P_{pi} - P_{pe}) . \quad (4.5-17)$$

By substituting the value of \bar{C}_{ba} found in (4.5-17) into (4.5-1), the value of \bar{P}_{ba} can be found.

V. PARAMETERS OF THE MODEL

This section assigns values to the various parameters of the model. The selected values have been "normalized" to fit a 1.6 kg bird. The description is of a female chicken (*Gallus Domesticus*) whenever possible and of a duck (*Cairina Moschata*) when the chicken data is unavailable. Thus the avian lung which is ultimately modeled is that of a hypothetical, 1.6 kg female bird resembling a chicken or duck.

5.1 Physical Parameters of the Lung

The parameters which define the model parabronchus are: ℓ , λ , α , ϕ , w . It has been necessary to infer these parameters from descriptions of the avian lung found in the literature which have been given in different terms.

The fractional distribution of lung volume for domestic fowl is given by Duncker [4] as shown below in Figure 7.

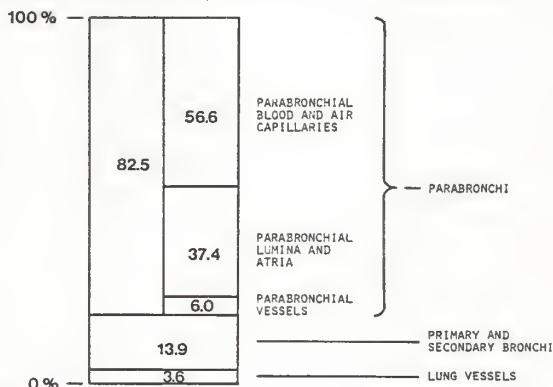


Figure 7. Fractional distribution of lung volume in domestic fowl (from Duncker, 1972)

Dunker also states that "... the air content of the lungs is estimated by taking the volume of the air conducting parts plus 50% of the blood air capillary net volume [4]." Hence, the air capillaries are taken to compose 50% of the volume of the parabronchial mantle.

Burton and Smith report that the air volume of both lungs of a 1.7 kg adult female chicken is 14.6 ml as determined by buoyancy on a recently killed specimen [7]. The adjusted value used here which is appropriate for a 1.6 kg bird is 13.74 ml.

From the data mentioned above, the total lung volume is determined to be

$$V_{\text{lung, total}} = \left[\frac{100}{(.374)(82.5) + (13.9) + (.5)(.566)(82.5)} \right] 13.74 \text{ ml} = 20.18 \text{ ml} .$$

The volume of all the parabronchi is

$$V_{\text{parabronchi}} = (.825)(20.18 \text{ ml}) = 16.64 \text{ ml} .$$

King and Cowie report that there may be 300-500 parabronchi in the lung of a chicken [8]. 400 parabronchi per lung are assumed here. The volume of a single parabronchus is

$$V_{\text{parabronchus}} = \frac{16.64 \text{ ml}}{800} = .0208 \text{ ml} .$$

The length of a parabronchus in a chicken or duck has not been found in the literature. But Dunker reports that the length of paleopulmonic parabronchi of a mute swan is 20-21 mm [5]. Based on this fact a length of 1.7 cm has been somewhat arbitrarily selected for the parabronchi of the model.

Although, cut in cross-section perpendicular to the axis a parabronchus appears hexagonal, for convenience, the parabronchi are here assumed circular in cross-section. The diameter of a parabronchus, d_p , including both the mantle and lumen is found from

$$\pi \left(\frac{d_p}{2} \right)^2 (1.7) = 0.208 \quad .$$

So, the parabronchial diameter is 0.1248 cm. The diameter of the parabronchial lumen, which is taken to include the atria, is found from

$$\pi \left(\frac{d_{pl}}{2} \right)^2 (1.7) = (.0208)(.374) \quad .$$

So, the parabronchial lumen diameter is 0.763 cm. The cross-sectional area of the parabronchial lumen is 0.00458 cm^2 . The mantle thickness is 0.0242 cm.

Air and blood capillaries penetrate the entire thickness of the mantle. Also, speaking of the blood capillaries in the mantle, Dunker states "... the length of the capillary stretch involved in exchange corresponds approximately to the thickness of the mantle of respiratory tissue of one parabronchus [4]." Hence, in the model presented here the length of the paired capillaries is taken to be 0.0242 cm.

Dunker reports the air capillary diameter in a domestic hen to be 0.001 cm [4]. The cross-sectional area of such an air capillary is $7.854 \times 10^{-7} \text{ cm}^2$ and the volume is $1.901 \times 10^{-8} \text{ cm}^3$. From the total lung volume occupied by air capillaries, and the volume of a single air capillary, the total number of air capillaries in both lungs is found to be

$$\frac{(.5)(.566)(16.64 \text{ ml})}{1.901 \times 10^{-8}} = 2.48 \times 10^8 \text{ capillaries} \quad .$$

The number of air capillaries associated with each parabronchus is

$$\frac{2.48 \times 10^8}{800} = 3.10 \times 10^5 \text{ capillaries per parabronchus} \quad .$$

The linear density of air capillaries along a parabronchus is

$$w = \frac{3.10 \times 10^5}{1.7} = 1.82 \times 10^5 \text{ capillaries per cm} \quad .$$

In summary, the physical parameters of the model parabronchus are taken to be

$$l = 0.0242 \text{ cm} ,$$

$$\lambda = 1.7 \text{ cm} ,$$

$$\alpha = 7.854 \times 10^{-7} \text{ cm}^2 ,$$

$$\phi = 4.580 \times 10^{-3} \text{ cm}^2 ,$$

$$\text{and } w = 1.82 \times 10^5 \text{ cm}^{-1} .$$

5.2 Blood Parameters

The O_2 capacity of avian blood used in this model is $7.2 \text{ mmol} \cdot \text{L}^{-1}$, which results from a Hb density of $120 \text{ gm} \cdot \text{L}^{-1}$ and an Hb capacity for O_2 of $0.060 \text{ mmol} \cdot \text{gm}^{-1}$. This value falls within the range reported by Scheipers et al. [9] of $6.7 \pm 1.3 \text{ mmol} \cdot \text{L}^{-1}$ for duck blood. Scheipers et al. [9] also display the in vivo O_2 dissociation curve for duck blood. For Cases 1, 2, 3, and 4 of the model it is necessary to approximate the sigmoid curve by a straight line, the slope of which is the value of β_{O_2} . This is done by assuming the straight line to pass through the 82 torr point representing arterial blood and the 39 torr point representing venous blood. The resulting slope, or solubility coefficient is

$$\beta = \frac{(0.91) - 0.43}{(82 - 39) \text{ torr}} \cdot 7.2 \text{ mmol} \cdot \text{L}^{-1} = 0.0804 \text{ mmol} \cdot \text{L}^{-1} \cdot \text{torr}^{-1} .$$

In Case 5 it is required that the O_2 dissociation curve be approximated, not by a straight line, but by a polynomial of second degree. This polynomial, giving partial pressure as a function of concentration, will have the general form

$$P = q_2 C^2 + q_1 C + q_0 .$$

The constants q_0 , q_1 , q_2 , which are to be chosen so that over the physiological range the polynomial accurately represents the dissociation curve, have been found by picking three points on the actual dissociation curve,

- 1) $P_1 = 81 \text{ torr}$, $C_1 = 6.55 \text{ mmol} \cdot \text{L}^{-1}$
- 2) $P_2 = 55$, $C_2 = 5.256$
- 3) $P_3 = 42$, $C_2 = 3.60$.

Substituting them into the general polynomial expression, obtaining three unknowns, and solving the equations for q_1 , q_2 , q_3 yields

$$q_0 = 92.29 \text{ torr} .$$

$$q_1 = -28.92 \text{ torr} \cdot \text{L} \cdot \text{mmol}^{-1} ,$$

and
$$q_2 = 4.152 \text{ torr} \cdot \text{L}^2 \cdot \text{mmol}^{-2} .$$

At the three chosen points the polynomial approximation will be exact; elsewhere in the physiological range it will be close to the real dissociation curve.

The effective in vivo dissociation curve, a linear approximation to it, and a polynomial approximation to it are illustrated in Figure 6. The linear approximation is a crude fit to the real dissociation curve over the physiological range. Between about 42 and 100 torr the polynomial provides a quite accurate approximation to the real dissociation curve. Above 100 torr the polynomial approximation tends toward oxygen concentrations which are slightly too high; below 42 torr the approximation and the real curve diverge widely.

The effective in vivo carbon dioxide dissociation curve for duck blood determined by Scheipers et al. [9] appears to be linear over the physiological range. They give the slope of that curve to be $\beta_{\text{CO}_2} = 0.27$

$\text{mmol}\cdot\text{L}^{-1}\cdot\text{torr}^{-1}$. It has not been attempted to find a polynomial approximation to the CO_2 dissociation curve for Case 5 of the model.

5.3 Diffusing Capacity of the Lung

By a carbon monoxide diffusing capacity test, Piiper, Pfeifer, and Scheid [10] determined the O_2 diffusing capacity of the lungs of 1.4 kg chickens to be $D_{\text{O}_2} = 1.0 \text{ ml}\cdot\text{min}^{-1}\cdot\text{torr}^{-1}$. The value to be taken for the model of the 1.6 kg bird is $1.14 \text{ ml}\cdot\text{min}^{-1}\cdot\text{torr}^{-1}$. This is in agreement with the value which Scheid and Piiper [2] determined by use of a model similar to the Case 1 developed here. From total lung diffusing capacity, total parabronchial mantle air volume, the air volume of a single capillary, and the length of an air capillary, it can be determined that the value of h , diffusing capacity per length along a single air capillary, is $h = 1.901 \times 10^{-7} \text{ ml}\cdot\text{min}^{-1}\cdot\text{torr}^{-1}\cdot\text{cm}^{-1}$. If mass is expressed in moles this becomes $h = 0.849 \times 10^{-8} \text{ mmol}\cdot\text{min}^{-1}\cdot\text{torr}^{-1}\cdot\text{cm}^{-1}$. The value used here for CO_2 diffusing capacity per length along a single air capillary is $1.698 \times 10^{-7} \text{ mmol}\cdot\text{min}^{-1}\cdot\text{torr}^{-1}\cdot\text{cm}^{-1}$, which is 20 times larger than the O_2 diffusing capacity.

5.4 Gas Parameters

The equation describing the diffusion of a single gas component in air written in terms of concentration is

$$\frac{dM}{dt} = -\alpha D \frac{dc}{dx} .$$

Written in terms of partial pressure it is

$$\frac{dM}{dt} = -\alpha \eta \cdot \frac{dP}{dx} ,$$

where

$$\eta = BD .$$

From the Handbook of Chemistry and Physics (reference [11]) are found the values

$$D_{O_2} = .178 \frac{\text{cm}^2}{\text{sec}}, \text{ and } D_{CO_2} = .139 \frac{\text{cm}^2}{\text{sec}}.$$

B is the solubility of a gas component in air.

$$B = \frac{1}{760} \frac{\text{ml}}{\text{ml} \cdot \text{torr}} = 5.874 \times 10^{-5} \frac{\text{mmol}}{\text{ml} \cdot \text{torr}}.$$

So,

$$\eta_{O_2} = 6.276 \times 10^{-4} \frac{\text{mmol}}{\text{min} \cdot \text{cm} \cdot \text{torr}},$$

and

$$\eta_{CO_2} = 4.899 \times 10^{-4} \frac{\text{mmol}}{\text{min} \cdot \text{cm} \cdot \text{torr}}.$$

These are the values assigned to the diffusion constants in the air spaces of both the parabronchial lumen and air capillaries.

5.5 Ventilation and Cardiac Output

It is reported by King and Payne [12] that the minute ventilation of a resting, unanesthetized 3.4 kg female chicken is 766 ml/min. Based on this data, the basal, resting value to be used for the 1.6 kg bird of this model is 360 ml/min.

Vogel and Sturkie [13] give values of cardiac output for female chickens. Based on their results, the value to be used here for basal, resting cardiac output of a 1.6 kg bird is 234 ml/min.

VI. RESULTS AND DISCUSSION

In Chapter III differential equations have been derived which describe the partial pressures of a diffusing gas component in the air capillaries, blood capillaries, and lumen of a model of the avian parabronchus. In Chapter IV solutions for these equations have been found. Evaluations of those solutions which will describe the performance of the model have been made, and they are presented graphically in this Chapter.

Figures 8A and 8B illustrate the partial pressures of oxygen along a blood capillary-air capillary pair which have been computed according to (4.3-27) and (4.3-29). A linear dissociation curve has been assumed and a finite diffusion coefficient has been used for the gaseous medium in the air capillary, these parameters taking the values which were arrived at in Chapter V. The air capillary has been assumed to open into parabronchial gas with $P_{O_2} = 160$ torr, this value giving a relatively great partial pressure difference between the blood and gas phases. Two cases have been considered for the state of the venous blood: $P_{O_2} = 20$ torr and $P_{O_2} = 40$ mmHg.

For the dotted curves of Figures 8A and 8B the cardiac output has been taken to be $\dot{Q} = 234$ ml/min, corresponding to the basal, resting rate. For both venous blood P_{O_2} values the end-capillary blood reaches an oxygen partial pressure of about 150 torr, coming to within 10 torr of complete equilibration with air capillary gas. In both cases the P_{O_2} in the air capillary varies only 0.3 torr along its entire length.

For the solid curves of Figures 8A and 8B the cardiac output has been increased to 2340 ml/min. For both venous blood P_{O_2} values the blood P_{O_2} rises only about 30 torr along the length of the capillary, increasing its

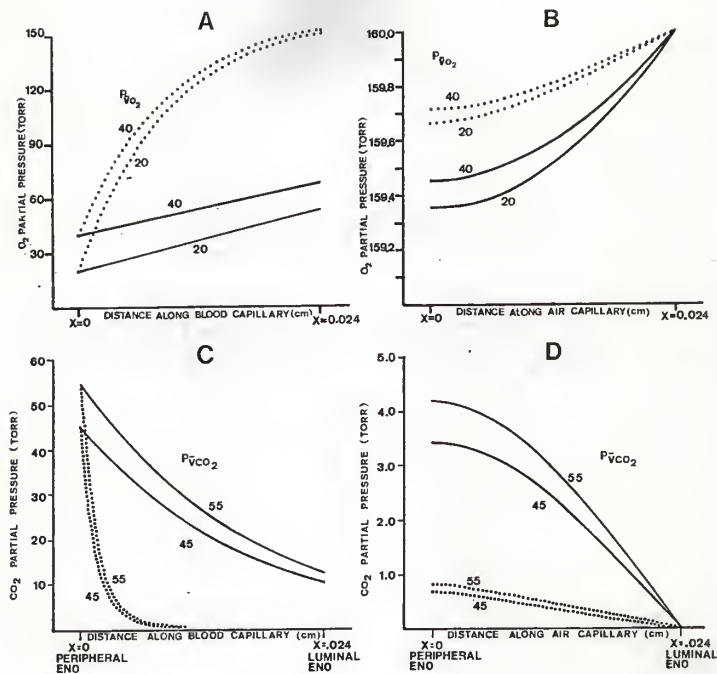


Figure 8. Partial pressures along a blood capillary and an air capillary when cardiac output is 234 ml/min (dotted lines) and when cardiac output is 2340 ml/min (solid lines). The cases considered for venous partial pressure are $P_{VO_2}=20$, $P_{VO_2}=40$, $P_{VCO_2}=45$, and $P_{VCO_2}=55$ torr. The luminal gas at the open end of the air capillary is described by $P_{O_2}=160$ and $P_{CO_2}=0$ torr. A: P_{O_2} along the blood capillary. B: P_{O_2} along the air capillary. C: P_{CO_2} along the blood capillary. D: P_{CO_2} along the air capillary.

partial pressure only about 25% of the way to full equilibration with air capillary gas. Since there is a greater difference between air capillary partial pressure and blood capillary partial pressure along the entire length of the capillary pair, a greater amount of oxygen diffuses into the blood from the air than in the case of $\dot{Q} = 234$ ml/min. The increased rate of oxygen diffusing into the air capillary then causes an increased oxygen partial pressure gradient along the length of the air capillary, causing a variation in oxygen partial pressure of about 0.6 torr along its entire length. Thus, increasing the rate of blood flow through the capillary by a factor of ten increases both the oxygen partial pressure gradient in the air capillary by a factor of approximately two and the rate of transfer of oxygen from the air capillary to the blood capillary by a factor of about two.

Figures 8C and 8D illustrate the partial pressures of carbon dioxide along the blood capillary-air capillary pair. Again, a linear dissociation curve and a finite diffusion coefficient have been used. The air capillary has been assumed to open into parabronchial gas with $P_{CO_2} = 0.0$ torr; the two cases considered for the state of venous blood are $P_{CO_2} = 45$ torr and $P_{CO_2} = 55$ torr; and the two cardiac outputs considered are $\dot{Q} = 234$ ml/min (dotted curves) and $\dot{Q} = 2340$ ml/min (solid curves). Observations similar to those made above for oxygen can also be made for carbon dioxide. Equilibration of blood with the gas phase occurs more readily at the lower cardiac output; the variation in carbon dioxide partial pressure along the length of the air capillary remains below 1.0 torr; and increasing the cardiac output by a factor of ten increases the air capillary partial gradient and rate of carbon dioxide transfer from blood to gas, both by a factor of approximately two.

In a brief analysis of diffusion in the air capillaries of a crow's lung, Hazlehoff [14] calculated that if the oxygen uptake of the bird is 2200 ml/min, the oxygen partial pressure difference between the ends of the capillary is about 19.0 torr. The oxygen uptake of his example is about 84 times that of the resting bird used in this research and his calculated partial pressure difference divided by 84 is .23 torr. This is a value very close to that arrived at here and illustrated in Figure 8B.

The very small variation in oxygen and carbon dioxide partial pressures along the air capillary implies that with only slight error the partial pressure of these gases can be regarded as essentially constant along the air capillary.

Figure 9A illustrates the variation of oxygen partial pressure along the parabronchus. Initially, the state of the gas is described by $P_{O_2} = 160$ torr. As the gas passes through the parabronchus oxygen diffuses through the blood-air capillary network into the blood causing the parabronchial partial pressure to decrease. Finally, the gas leaves the parabronchus with a lower oxygen partial pressure than it entered with. At fixed cardiac output of 234 ml/min ventilation rates from 18 to 720 ml/min have been assumed and the state of venous blood is described by $P_{O_2} = 40$ torr.

Assuming a given average ventilation for the lungs, at any instant the individual members of the population of parabronchi in the lungs of a real bird will experience a spread of ventilatory rates both above and below the average rate. Also, the ventilation of the parabronchi will vary second by second through the different phases of the respiratory cycle. For these reasons different gas flow rates through the parabronchi are of interest even at a constant, average whole-lung ventilation rate.

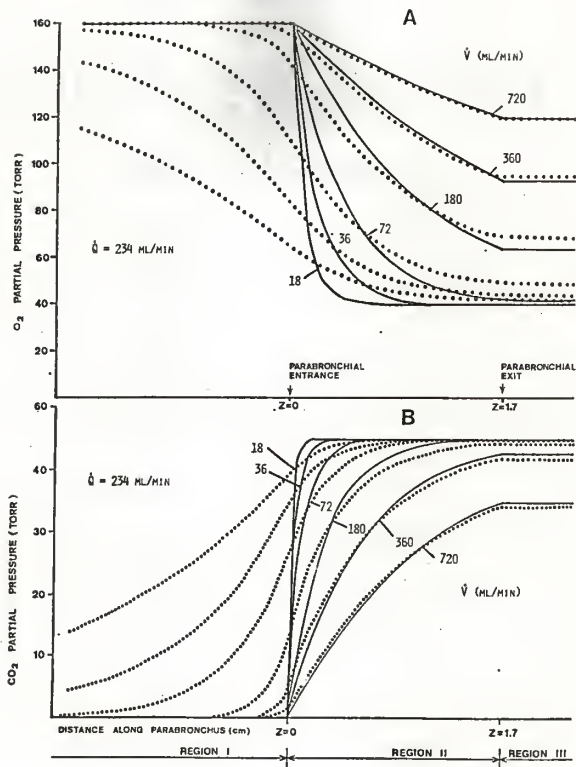


Figure 9. Partial pressures along the parabronchus computed under the assumption of (1): equal diffusion resistance in the air capillaries and parabronchial lumen (dotted curves) and, (2): constant partial pressure along the air capillaries and bulk flow only in the parabronchial lumen (solid curves). The ventilation varies from 18 to 720 ml/min. The state of inspired gas is $P_{iO_2}=160$ and $P_{iCO_2}=0$ torr; the state of venous blood is $P_{VO_2}=40$ and $P_{VCO_2}=45$ torr. A: P_{O_2} along the parabronchus. B: P_{CO_2} along the parabronchus.

For the solid curves of Figure 9A it has been assumed that the gas moves by bulk flow without any diffusion either forward or backward in the axial direction. This is the assumption of Case 1, and these curves have been calculated according to (4.3-11). It can be seen that at the slower rates, better equilibration of parabronchial gas with the venous blood is achieved. Another obvious characteristic of these curves is that they indicate no change in the partial pressure of the gas until it physically enters the parabronchus.

For the dotted curves of Figure 9A movement of gas through the parabronchus both by bulk flow and by diffusion in the axial direction have been accounted for. These results have been calculated according to (4.4-11) and (4.4-12). The most remarkable characteristic of these curves is that they indicate a change in the partial pressure of the gas before it physically enters the parabronchus. This is due to the gas which has not yet reached the parabronchus diffusing toward the region of lowered oxygen partial pressure within the parabronchus.

At high ventilation rates bulk flow is relatively much more important than diffusion, so diffusion can be neglected with only a slight error being introduced. At lower ventilation rates diffusion becomes more important, and the partial pressure variation along the parabronchus is not well approximated by the solid curves of Figure 9A in which diffusion is neglected. If, however, one is interested not in the partial pressure profile along the parabronchus, but only in the overall rate of oxygen exchange taking place in the parabronchus, it appears not to matter very much whether diffusion is accounted for or not. This conclusion follows from a comparison, at a given ventilation rate, of the end-parabronchial partial pressure values in Figures 9A and 9B which reveals only a small difference.

Figure 9B illustrates the variation of carbon dioxide partial pressure along the parabronchus. The gas approaching the parabronchus is assumed initially to have $P_{CO_2} = 0.0$ torr; the venous blood is assumed to have $P_{CO_2} = 45$ torr; the cardiac output is assumed fixed at 234 ml/min; and a range of ventilation rates from 18 to 720 ml/min is considered. For the solid curves diffusion is neglected; for the dotted curves diffusion is taken into account. The same conclusions which were arrived at in the consideration of oxygen also apply to these carbon dioxide curves.

The attempt is made in the discussion of Figures 10A and 10B to give a more complete picture of the whole parabronchus as a gas exchange device by combining the results describing partial pressure variation along the blood capillaries with those describing the variation along the parabronchial lumen. Figure 10A treats oxygen; Figure 10B treats carbon dioxide. The series of curves on the left describes partial pressure variation in blood capillaries which are located at different positions along the parabronchus. In each capillary the partial pressure changes from the venous value to the end-capillary value, the rate and extent of that rise depending on the partial pressure of the gas in the adjacent air capillary. The partial pressure in the air capillary depends upon the partial pressure in the parabronchial gas into which the air capillary opens, which in turn depends upon its location along the parabronchus. The variation in partial pressure of the gas along the parabronchus is shown by the curve on the right. The physical location of a blood capillary with respect to position along the parabronchus is indicated by the dotted lines. The vertical segment of the dotted line indicates the extent to which the capillary blood falls short of full equilibration with the gas in the adjacent air capillary. The gas leaving the parabronchus is at the partial pressure indicated by the right

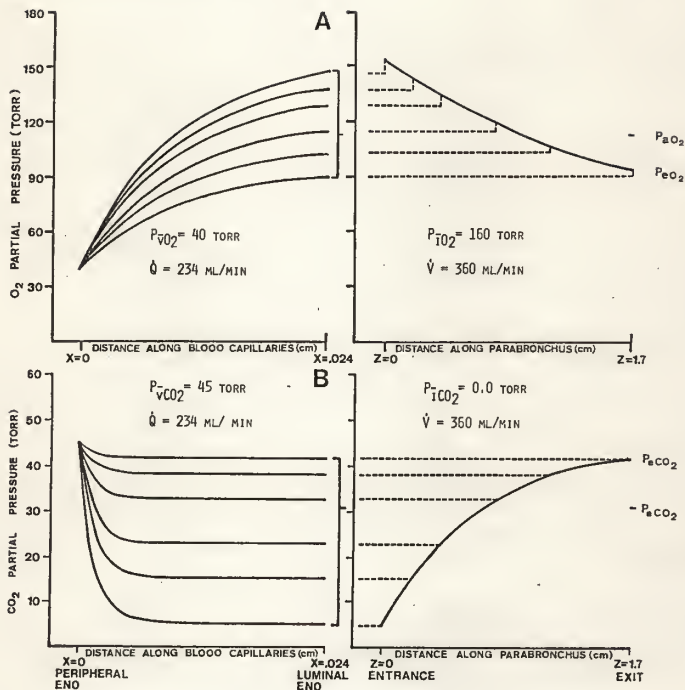


Figure 10. A: O_2 partial pressure along several parabronchial blood capillaries (left) and along the parabronchial lumen (right). The capillary location along the parabronchus is indicated by horizontal dotted lines. The extent to which blood falls short of full equilibration with air is indicated by vertical dotted lines. B: CO_2 partial pressure along several parabronchial blood capillaries and along the parabronchial lumen.

end point of the parabronchial gas curve. The arterial blood is formed from the blood emptying out of all the blood capillaries along the parabronchus, so the partial pressure of the arterial blood is some average of the values of partial pressure of the right end points of the blood capillary curves.

The results illustrated in Figures 8 through 10 have all been based upon the assumption of a linear dissociation curve. This is reasonable when considering carbon dioxide, but not when considering oxygen. A consequence of the linear dissociation curve used in the model so far is that when the partial pressure of oxygen in blood climbs above about 100 torr, the concentration of oxygen in blood rises above the real physiological limits. Calculations based upon the model with a linear dissociation curve can exaggerate the rate at which oxygen is transferred from the gas phase to the blood phase. The oxygen concentration in the arterial blood can be too high and the partial pressure of oxygen in the end-parabronchial gas can be too low.

To obtain more accurate results for oxygen exchange, Case 5 of the model has been developed in which the non-linearity of the oxygen dissociation curve has been taken into account. Based on Case 5, Figure 11 illustrates the variation of oxygen partial pressure in the blood capillaries at different locations along the parabronchus and the variation of oxygen partial pressure in the parabronchial gas. The ventilation rate has been taken to be 360 ml/min; the cardiac output, 234 ml/min; the partial pressure of venous blood, 43 torr. The reason for increasing the partial pressure of venous blood in Case 5 is to keep on the right limb of the approximate dissociation curve illustrated in Figure 6. Figure 12, also calculated

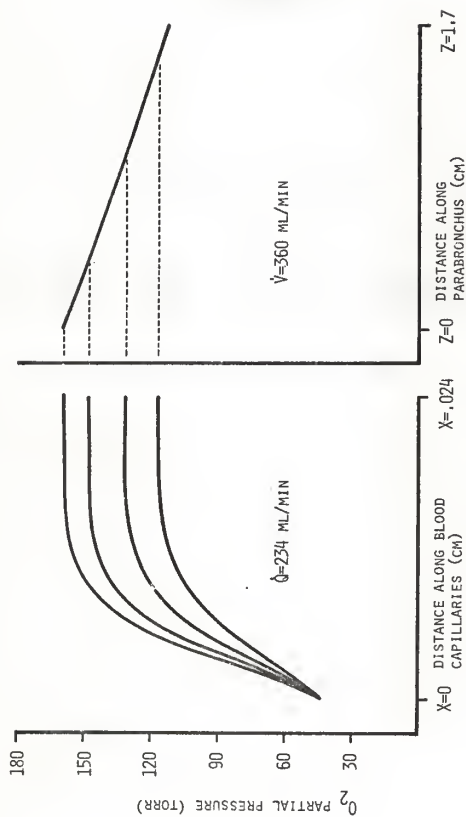


Figure 11. O_2 partial pressures along blood capillaries and parabronchus computed with a non-linear dissociation curve. Cardiac output=234 ml/min; ventilation=360 ml/min.

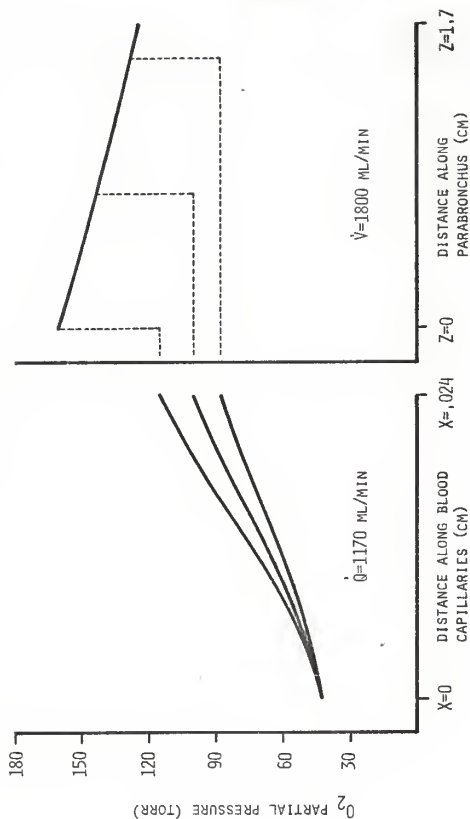


Figure 12. O_2 partial pressures along blood capillaries and parabronchus computed with a non-linear dissociation curve. Cardiac output=1170 ml/min; ventilation=1800 ml/min.

from Case 5, is similar to Figure 11, but the ventilation rate and the cardiac output are 1800 ml/min and 1170 ml/min, respectively. Figures 13A and 13B illustrate the oxygen concentration in the same blood capillaries under the same conditions as in Figures 11 and 12, respectively.

Comparison of Figures 10A and 11 reveals some interesting differences. In Figure 10A the curves describing the rise of oxygen partial pressure in the blood capillaries have the character of a decaying exponential. In Figure 11 the blood capillary curves rise faster initially to a knee, then form a plateau where they are almost level. Also, in Figure 11 the capillary blood appears to equilibrate more completely with the gas phase. The curve in Figure 11 describing oxygen partial pressure of parabronchial gas does not fall to an end-parabronchial value as low as that of Figure 10A. This is a direct consequence of the blood with a more realistic, non-linear dissociation curve becoming saturated. Thus, less oxygen is extracted from the parabronchial gas.

When ventilation rate and cardiac output are increased five-fold, as shown in Figure 12, the capillary blood is quite far from full equilibration with the gas phase by the end-capillary point and the oxygen partial pressure of the gas phase does not drop so far by the end-parabronchial point.

From Figure 13 it can be seen that at the basal, resting ventilation rate and cardiac output the oxygen concentration of capillary blood rises quickly to a plateau and increases only slightly thereafter. When the flow rates are increased by a factor of five the oxygen concentration in the blood capillaries rises steadily along the entire capillary length and reaches the end-capillary point in a nearly, but not completely, saturated condition.

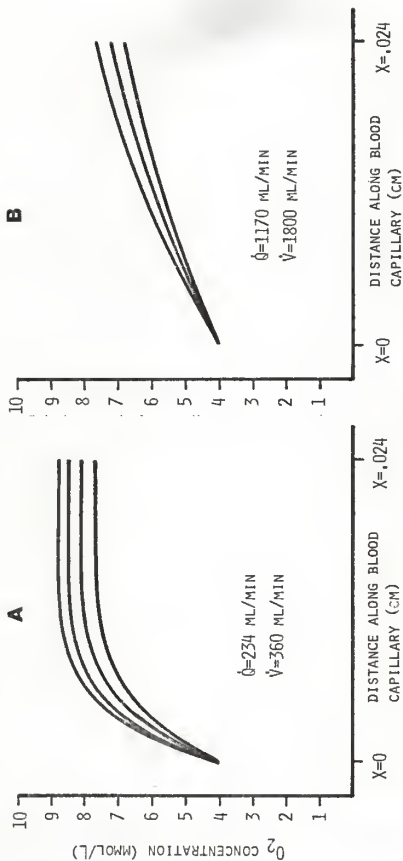


Figure 13. O_2 concentrations along blood capillaries computed with a non-linear dissociation curve. A: Cardiac output=234 ml/min; ventilation=360 ml/min.

B: Cardiac output=1170 ml/min; ventilation=1800 ml/min.

Figure 14 shows the oxygen partial pressure, calculated from Case 5, of the end-parabronchial gas under different conditions of ventilation and cardiac output. The inspired gas is assumed to have $P_{O_2}=160$ torr, and the venous blood is assumed to have $P_{O_2}=43$ torr. The trends are what one would expect intuitively. Increasing ventilation rates gives the gas less chance to equilibrate with blood, so the end-parabronchial oxygen partial pressure increases. Decreasing cardiac output causes the gas to be exposed to more fully saturated blood on the average, again causing end-parabronchial oxygen partial pressure to increase.

Recall that blood exiting from all the different capillaries in the lung at many different states of saturation mixes together to form the arterial blood. Figures 15 and 16 illustrate the arterial oxygen partial pressure and concentration, respectively, which have been calculated according to Case 5, under different conditions of ventilation and cardiac output. Increasing cardiac output decreases saturation of arterial blood, and increasing ventilation increases the saturation.

Increasing cardiac output results in an increased quantity of oxygenated blood carried from the lung to the tissues; however, increasing cardiac output causes that blood which is carried to contain less oxygen. So, what is the net effect? What happens to oxygen uptake?

An elementary argument forces one to conclude that, if the partial pressures of the venous blood and inspired air entering the lung are fixed at constant, unvarying values, then increasing the rate of flow of either blood or gas must increase the rate of oxygen uptake by the blood. Increasing the rate of flow of blood or gas through the lung will decrease the equilibration between blood and gas. This decreased equilibration will result in greater partial pressure differences across the exchange surfaces

of the lung, which will in turn cause a greater rate of oxygen transfer across those exchange surfaces. That is, greater oxygen uptake.

The model, Case 5 with the approximate, non-linear dissociation curve, has been used to compute oxygen uptake at various values of ventilation rate and cardiac output. The range is from basal, resting rates up to eight times normal for both blood and gas. The inspired gas has $P_{O_2}=160$ torr and the venous blood has $P_{O_2}=43$ torr. The results are shown in Figure 17.

From Figure 17 it is seen that the greatest increase in oxygen uptake is achieved by increasing both cardiac output and ventilation as much as possible. An interesting result displayed by Figure 17 concerns small increases in oxygen uptake. Starting from basal flow rates, increasing the ventilation while keeping cardiac output constant causes a negligible increase in oxygen uptake. However, increasing the cardiac output while keeping ventilation constant causes a very significant increase in oxygen uptake. This result is explainable. At the basal flow rates blood that leaves the lung is almost fully oxygenated. Increasing the ventilation will not significantly increase the level of oxygenation of the blood, so the oxygen uptake cannot increase significantly. But increasing the cardiac output will cause an increased amount of blood that is fully oxygenated, or nearly so, to be carried from the lung to the tissues.

By drawing a horizontal line across Figure 17 at a particular level of oxygen uptake one can see that there is an infinite number of combinations of gas and blood flow rates that will satisfy that level of oxygen uptake. This model does not select any one of those as more preferable than the others. It would be interesting to determine experimentally which points on such a graph an exercising bird selects.

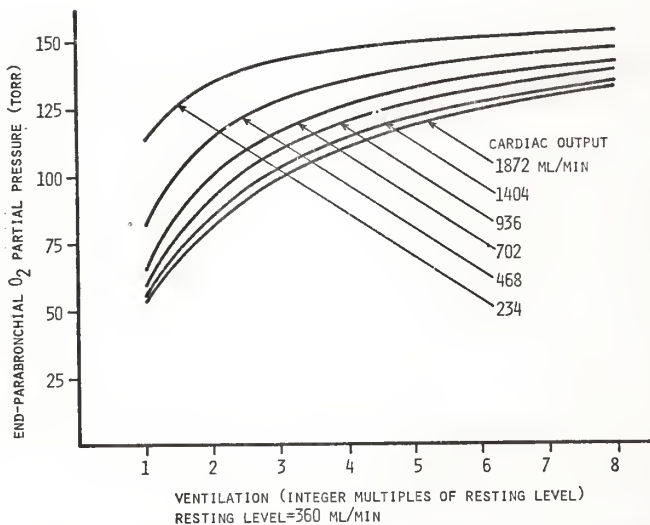


Figure 14. Dependence of end-parabronchial O_2 partial pressure on cardiac output and ventilation. A non-linear O_2 dissociation curve is used.

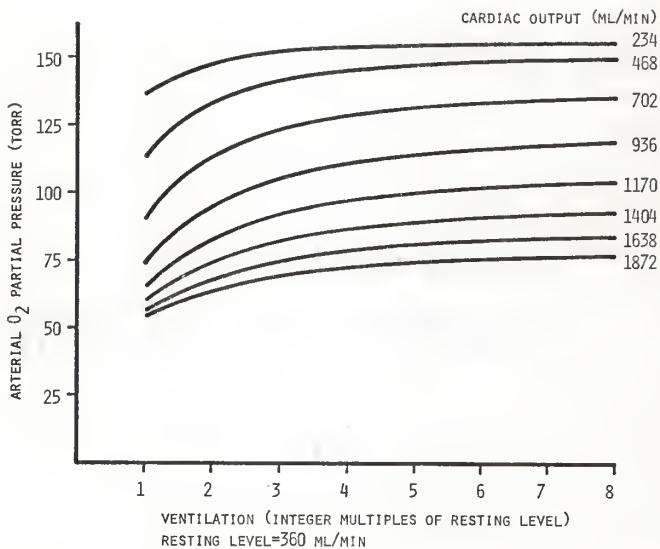


Figure 15. Dependence of arterial O_2 partial pressure on cardiac output and ventilation. A non-linear O_2 dissociation curve is used.

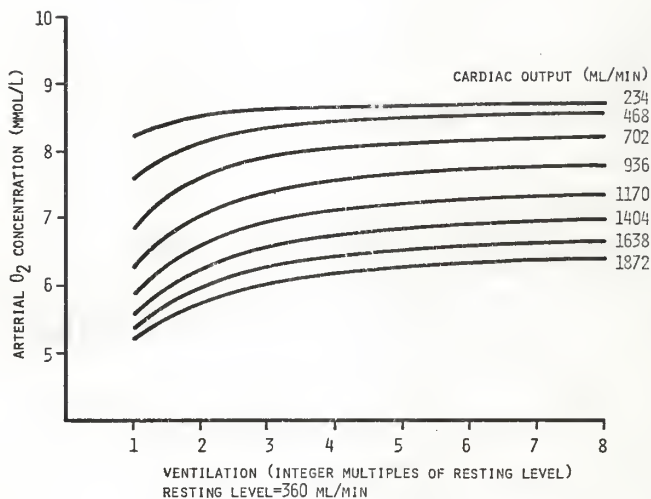


Figure 16. Dependence of arterial O_2 concentration on cardiac output and ventilation. A non-linear O_2 dissociation curve is used.

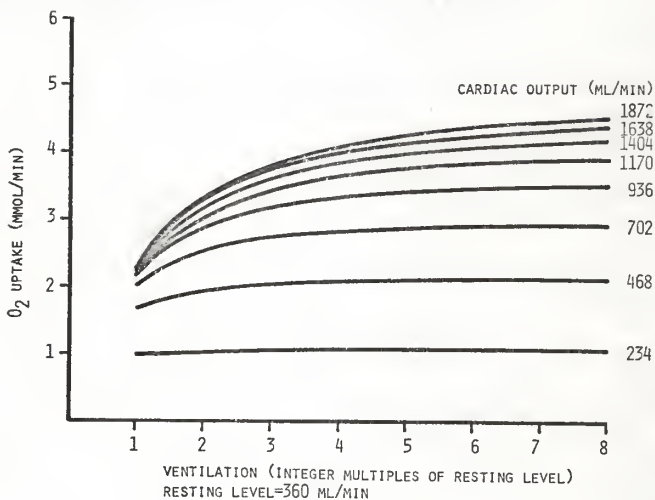


Figure 17. Dependence of O₂ uptake on cardiac output and ventilation. A non-linear O₂ dissociation curve is used.

The maximum increase in oxygen uptake shown in Figure 17 is about 4-1/2 times above the basal level. This occurs when blood and gas flow rates are increased eight times above their basal levels. This may seem low. The model, however, assumes a constant level of venous blood oxygen partial pressure regardless of cardiac output and ventilation rate, which is a condition that probably does not hold in a real bird. But the venous oxygen partial pressure levels are determined by the metabolic rates of the tissues and the model constructed here is a model of the lung only. If the venous blood were to take a lower value for oxygen partial pressure, which the Case 5 model in its present form cannot accommodate, the oxygen uptake might be boosted toward a level that better simulates exercise conditions.

As ventilation rate and cardiac output increase, the average oxygen partial pressure of the gas exposed to the exchange surfaces of the lung approaches that of fresh, inspired air, and the average partial pressure of the blood exposed to those surfaces approaches that of venous blood. So an upper limit on oxygen uptake can be calculated by assuming the exchange surfaces to be completely exposed to venous blood on one side and fresh air on the other. The oxygen uptake under these hypothetical conditions is calculated by multiplying the total diffusing capacity of the lungs times the difference in partial pressure between the blood and gas phases. Results are shown in Figure 18 for a range of oxygen partial pressures in the blood and an oxygen partial pressure of 160 mmHg in the gas. The diffusing capacity has been taken to be $.0509 \text{ mmol} \cdot \text{min}^{-1} \cdot \text{torr}^{-1}$.

In considering the oxygen uptake increases shown in Figure 17 it should also be remembered that the lung parameters used in this model are

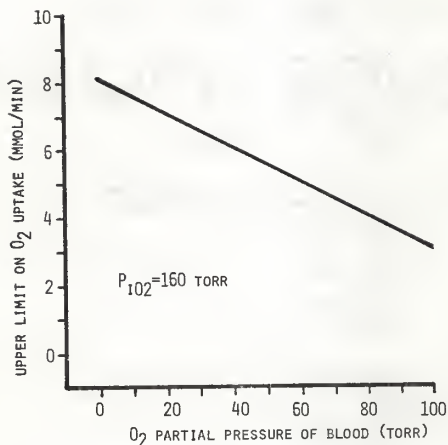


Figure 18. Upper limit on O_2 uptake by the lungs as a function of venous O_2 partial pressure. O_2 partial pressure of inspired gas is $P_{iO_2}=160$ torr.

those of a female chicken, a bird which may not be able to achieve a high oxygen uptake. In particular, the air capillaries of other birds have a smaller diameter than .001 cm, reaching as low a dimension as .0003 cm in some species (Dunker [4]). Smaller air capillaries increase the diffusing capacity of the lung, which in turn increase the maximum oxygen uptake.

Kawashiro and Scheid [15] report that in resting, unanesthetized hens the oxygen partial pressure of arterial blood is 82 torr. The results obtained here from the model indicate a much higher arterial oxygen partial pressure in resting birds. Since under resting conditions maximum oxygenation of blood should be obtained in the real bird as well as in the model, this discrepancy presents a challenge to the assumptions upon which the model is based. Two effects which the model does not take into account are the shunting of blood past the lung without an opportunity to undergo gas exchange and the presence of ventilation-perfusion imbalances, whatever may be the form they assume in an avian lung.

In a real bird some blood may be shunted past the lung without being exposed to the gas exchange surfaces. Under basal conditions that blood which is not shunted will undergo gas exchange leaving the parabronchi at $P_{O_2} = 140$ torr and $C_{O_2} = 8.25$ mmol/L. Its state is described by a point far up the dissociation curve of Figure 6. Mixing with a small amount of shunted blood will reduce the oxygen concentration slightly, but because of the slope of the dissociation curve the partial pressure will be greatly reduced, perhaps to 82 torr. Ventilation-perfusion imbalances should have a similar effect.

VII. RECOMMENDATIONS FOR FUTURE WORK

A logical project with which to follow up this thesis would be an experiment having the dual objectives both of testing the accuracy of the model and, if it proves sufficiently accurate, of determining possible locations of the CO_2 receptors in the avian lung.

To test the model it would be necessary to unidirectionally ventilate the lung, as discussed in reference [3], of a species having negligible neopulmo and to record cardiac output, ventilation, and partial pressures of inspired and expired gas and of venous and arterial blood. Comparison of these recorded values with those predicted by the model would indicate the validity of the model.

To determine possible receptor locations, it would be necessary to first "calibrate" the receptor's sensitivity to carbon dioxide partial pressure by taking recordings from the vagus nerve. Then, when the lung is unidirectionally ventilated the recordings from the vagus nerve will indicate the CO_2 partial pressure in the microenvironment of the receptor and the model will indicate which locations are compatible with that partial pressure.

Another possible experiment, alluded to in Chapter VI, would be to record from a bird the levels of cardiac output and ventilation under different conditions of oxygen uptake. Since these two variables can be combined in an infinite number of ways to yield the same oxygen uptake, it would be interesting to see which combination is actually selected by a particular bird.

Future work on the model itself could include the addition of a compartment, or compartments, to represent the body tissues. Within

such a compartment the blood would lose oxygen and gain carbon dioxide. In this way the partial pressures in the venous blood would not have to be set arbitrarily, but would be determined within the model itself and would be dependent upon the constraints placed on the model.

The accuracy of Case 5 of the model could be improved by using a third order polynomial representation of the oxygen dissociation curve, instead of a second order representation as has been done in this research.

ACKNOWLEDGEMENT

The author gratefully acknowledges the members of his graduate committee, Dr. Richard R. Gallagher, Dr. Marion R. Fedde, and Dr. Nasir Ahmed, for the guidance and constructive criticism they have provided during the research and preparation of this thesis. Special thanks are extended to Dr. Richard R. Gallagher, who served as major professor, for providing the opportunity to investigate the modeling of systems in respiratory physiology and to Dr. Marion R. Fedde, who suggested that the respiratory system which was modelled be avian.

Also, the author is grateful to Dr. Randall N. Gatz for assistance in formulating the publication manuscript.

Thanks are owed to Jan Gaines for typing, to Mr. John Schmalzel for assistance in preparation of the figures, and to teaching resources in the College of Veterinary Medicine for assistance in preparation of the figures.

This research was supported by NIOSH Bioenvironmental Engineering Training Grant No. 5T01-OH00024-08.

REFERENCES

1. Zeuthen, E.: The ventilation of the respiratory tract in birds. Kgl. Danske Videnskab. Selskab Biol. Medd., 17:1-50 (1942).
2. Scheid, P., Piiper, J.: Analysis of gas exchange in the avian lung: theory and experiments in the domestic fowl. Respir. Physiol. 9:245-262 (1970).
3. Fedde, M. R., Gatz, R. N., Slama, H., Scheid, P.: Intrapulmonary CO₂ receptors in the duck: I. Stimulus specificity. Respir. Physiol. 22: 99-114 (1974).
4. Dunker, H. R.: Structure of avian lungs. Respir. Physiol. 14:44-63 (1972).
5. Dunker, H. R.: Structure of the avian respiratory tract. Respir. Physiol. 22:1-19 (1974).
6. Bois, G. Petit: "Tables of Indefinite Integrals," Dover Publications, Inc., New York, 1961.
7. Burton, R. R., Smith, A. H.: Blood and air volumes in the avian lung. Poultry Sci. 47:85-91 (1968).
8. King, A. S., Cowie, A. F.: The functional anatomy of the bronchial muscle of the bird. J. Anat. 105:323-336 (1969).
9. Scheipers, G., Kawashiro, T., Scheid, P.: Oxygen and Carbon dioxide dissociation of duck blood. Respir. Physiol. 24:1-13 (1975).
10. Piiper, J., Pfeifer, K., Scheid, P.: Carbon monoxide diffusing capacity of the respiratory system in the domestic fowl. Respir. Physiol. 6:309-317 (1969).
11. Handbook of Chemistry and Physics. 49th edition (1968), pg. F47.
12. King, A. S., Payne, D. C.: Normal breathing and the effects of posture in Gallus Domesticus. J. Physiol. (London) 174:340-347 (1964).
13. Vogel, J. A., Sturkie, P. D.: Cardiovascular responses on chicken to seasonal and induced temperature changes. Science. 140:1404-1406 (1963).
14. Hazelhoff, E. H.: Bouw en functie van de vogellong. Versl. gewone Vergad. Afd. Natuurk. Kon. Ned. Akad. Wst. 52:391-400 (1943).
English translation: Structure and function of the lung of birds. Poultry Sci. 30:1-30 (1951).
15. Kawashiro, T., Scheid, P.: Arterial blood gases in undisturbed resting birds: measurements in chicken and duck. Respir. Physiol. 23:337-342 (1975).

APPENDIX A

Definitions of symbols

x	location along either capillary (cm)
z	location along the parabronchus (cm)
l	length of capillaries (cm)
λ	length of the parabronchus (cm)
α	cross sectional area of an air capillary (cm^2)
ϕ	cross sectional area of the parabronchus (cm^2)
w	capillary density along a parabronchus (cm^{-1})
P_b	partial pressure in the blood capillary (torr)
P_g	partial pressure in the air capillary (torr)
P_{bn}	partial pressure in the n^{th} cell of the blood capillary (torr)
P_{gn}	partial pressure in the n^{th} cell of the air capillary (torr)
P_{bv}	partial pressure in venous blood entering blood capillary (torr)
P_{ba}	partial pressure in blood leaving blood capillary (torr)
\bar{P}_{ba}	partial pressure in blood leaving parabronchus (torr)
P_{gp}	partial pressure in air capillary at open end (torr)
$\frac{dP}{dx} \frac{gP}{gP}$	derivative of P_g at open end ($\text{torr} \cdot \text{cm}^{-1}$)
P_p	partial pressure in the parabronchus (torr)
P_{pi}	partial pressure in air entering parabronchus (torr)
P_{pe}	partial pressure in air leaving parabronchus (torr)
C	concentration. It has the same subscripting as P ($\text{mmol} \cdot \text{L}^{-1}$)
f	rate of blood flow in blood capillary ($\text{L} \cdot \text{min}^{-1}$)
β	solubility coefficient in blood capillary ($\text{mmol} \cdot \text{L}^{-1} \cdot \text{torr}^{-1}$)

h	diffusing capacity between blood and air capillaries per unit length ($\text{mmol} \cdot \text{min}^{-1} \cdot \text{torr}^{-1} \cdot \text{cm}^{-1}$)
F	rate of gas flow in the parabronchus ($\text{L} \cdot \text{min}^{-1}$)
B	solubility coefficient in parabronchus ($\text{mmol} \cdot \text{L}^{-1} \cdot \text{torr}^{-1}$)
η	diffusion constant in air capillary ($\text{mmol} \cdot \text{min}^{-1} \cdot \text{cm}^{-1} \cdot \text{torr}^{-1}$)
θ	diffusion constant in parabronchus ($\text{mmol} \cdot \text{min}^{-1} \cdot \text{cm}^{-1} \cdot \text{torr}^{-1}$)
\dot{Q}	total blood flow to a parabronchus ($\text{L} \cdot \text{min}^{-1}$)
\dot{Q}_v	flow of blood which has not yet undergone exchange at same location along the parabronchus ($\text{L} \cdot \text{min}^{-1}$)
\dot{Q}_a	flow of blood which has undergone gas exchange at some location along the parabronchus ($\text{L} \cdot \text{min}^{-1}$)

APPENDIX B

Publication Manuscript: Theory of Gas Exchange in the Avian Parabronchus."
William D. Crank and Richard R. Gallagher

ABSTRACT. To understand the distribution of oxygen and carbon dioxide in the avian lung, a theoretical treatment of gas exchange in the parabronchus of the avian lung is described. The model used is modified after Zeuthen (1942). In addition to bulk flow through the parabronchial lumen, mass transport by diffusion through the air spaces of both the parabronchial lumen and air capillaries is treated. The relationship of the partial pressures of oxygen and carbon dioxide within the blood capillaries, air capillaries, and parabronchial lumen to parabronchial blood flow and ventilation is graphically shown.

The results indicate that the maximum partial pressure variations of oxygen and carbon dioxide along the length of an air capillary are less than one torr and five torr, respectively. Also, the resistance to gas exchange imposed by diffusion across the blood-gas interface is many times greater (about 250 times greater for O_2 ; ranging from 8.5 to 33 times greater for CO_2) than the resistance imposed by diffusion through the air capillaries. The assumption of bulk flow only through the parabronchial lumen yields accurate results at resting and high ventilation rates, but axial diffusion in the lumen must additionally be considered at lower ventilation rates. Before physically entering the parabronchus, the gas in the pre-parabronchial region shows a reduction in O_2 partial pressure due to forward diffusion toward the parabronchus and an increase in CO_2 partial pressure due to backward diffusion from the parabronchus. Also, the way in which the respiratory exchange ratio varies with position along the parabronchus is shown.

INTRODUCTION

The avian respiratory system, in contrast to that of mammals or reptiles, has rigid lungs in which gas is exchanged and air sacs which act as bellows to ventilate those lungs. The parabronchi, numbering in the hundreds, are the functional units of each lung. Each parabronchus is basically a cylindrical structure penetrated by a lumen along its central axis. Ventilated gas passes down the lumen, and loses oxygen and picks up carbon dioxide. Oxygen diffuses into the air capillaries, which radiate outward from the parabronchial lumen, and carbon dioxide diffuses in the opposite direction. Within an air capillary there is no bulk flow of gas (Zeuthen, 1942). Gas is exchanged across the surfaces separating air capillaries from the adjacent blood capillaries. The direction of flow through the blood capillaries is from the parabronchial periphery inward toward the parabronchial lumen (Abdalla and King, 1974; West, Bamford, and Jones, 1977). Venous blood enters the capillaries at the periphery and the blood leaving the capillaries mixes to form arterial blood.

Scheid and Piiper (1970) developed a cross-current model to describe the function of the avian parabronchus. In their model, gas is exchanged between the gas moving by bulk flow through a tube and a thin sheet of blood flowing across the surface of that tube. The direction of blood flow is perpendicular to the direction of gas flow, which is the reason they describe the model as "cross-current."

In the cross-current model it is assumed that the partial pressure of O_2 or CO_2 is constant throughout a cross-section cutting the tube perpendicular to its axis. Applied to the avian parabronchus, this

assumption forces the partial pressure along the radially projecting air capillaries to be constant, which implies zero diffusion resistance. It is also assumed that gas moves through the parabronchial lumen only by bulk flow without axial diffusion, which implies infinite diffusion resistance. Diffusion through the air spaces must occur, however, with equal resistance in both the radial and axial directions if a square velocity profile across the lumen is assumed.

In the model described here, the blood and air capillaries are retained as separate structures. Also, the diffusion constant of O_2 or CO_2 in air characterizes the diffusion radially along the air capillaries and axially along the lumen. Constant partial pressure is still assumed for a cross section through the lumen.

THEORY

The physical structure of the model is shown in Figure 1A. This representation is similar to that of Zeuthen (1942). Explicitly, the more important assumptions of the model are: 1) Steady state operation, 2) Homogeneous perfusion of the parabronchus, 3) Homogeneous exchange surface between gas and blood, 4) Linear O_2 and CO_2 dissociation curves, 5) No interaction between O_2 and CO_2 , 6) Square velocity profile across the parabronchial lumen.

All the blood which exchanges gas with a given air capillary is taken to flow through a single, adjacent blood capillary. It is assumed that the air capillaries are the same length as the blood capillaries. Both air and blood capillaries are represented as a series of homogeneous compartments of length Δx with mass transport across compartment surfaces. The expressions describing this transport between

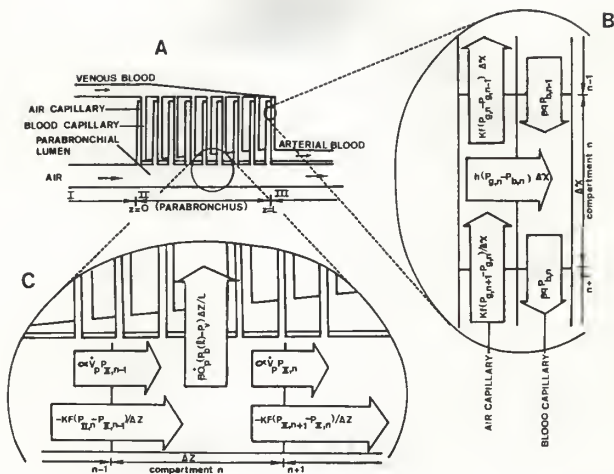


Figure 1. A: The parabrachial model, modified after Zeuthen. B:

Detail of air capillary and blood capillary compartments. Expressions describing transport of the considered gas between compartments are shown. C: Detail of parabrachial luminal compartments. Expressions are shown which describe transport between luminal compartments by both bulk flow and diffusion and transport between a luminal compartment and the air capillaries which open into it.

compartment n and the adjacent compartments are shown in Figure 1B. The symbols used are defined in Appendix C. In a single air or blood capillary compartment, equating the influx of the considered gas to the efflux yields a difference equation. Performing the limit $\Delta x \rightarrow 0$ transforms this into a differential equation. In Appendix A the derivation of differential equations for air capillary and blood capillary partial pressures and the boundary conditions on the solutions of those equations are given in detail.

Illustrated in Figure 1A are three regions, denoted I, II, and III, through which the parabronchial gas consecutively flows. The parabronchus is coincident with region II. The parabronchial entrance and exit lie at $z=0$ and $z=L$. Although this geometry only approximately depicts the opening of a parabronchus into a secondary bronchus, the results should give some insight into the gas transport processes occurring there.

By a compartmentalization similar to that of the air and blood capillaries, the parabronchial lumen is considered to be composed of a series of homogeneous compartments of length Δz . Transport between compartment n , adjacent compartments, and the air capillaries is illustrated in Figure 1C. The transport due to bulk flow is shown separately from that due to diffusion. The transport due to all the air capillaries opening into the compartment accounts for the gas exchanged between the blood phase and gas phase. In a single parabronchial compartment, equating the influx of the considered gas to the efflux and performing the limit $\Delta z \rightarrow 0$ yields a differential equation for partial pressure along the parabronchus. The differential equations for partial pressure in regions I, II, III and the boundary conditions on their solutions are given in Appendix A.

In Appendix B the differential equations are solved for the partial pressure in the air capillaries, blood capillaries and regions I, II, III along the parabronchial lumen.

RESULTS

The partial pressures of O_2 and CO_2 along a blood capillary and an air capillary have been calculated from equations (29) and (30) of Appendix B. Figure 2A illustrates that within a blood capillary the O_2 partial pressure increases from the venous end at the parabronchial periphery ($X=0$) to the arterial end at the parabronchial lumen ($X=0.024$). Figure 2B illustrates that within an air capillary the O_2 partial pressure increases from the closed end at the periphery ($X=0$) to the open end at the lumen ($X=0.024$). This gradient forces O_2 to diffuse from the lumen into the air capillary. Figure 2C shows the decrease of CO_2 partial pressure from the venous end to the arterial end of the blood capillary. Figure 2D illustrates the decrease of CO_2 partial pressure from the peripheral end to the luminal end of the air capillary. This gradient forces CO_2 to diffuse from the air capillary into the lumen.

In Figure 2 the air capillary has been assumed to open into parabronchial gas with $P_{O_2}=160$ and $P_{CO_2}=0$ torr. Two cases have been considered for the parabronchial perfusion: $\dot{Q}_p=0.29$ and $\dot{Q}_p=2.9$ ml/min. Two cases have been considered for the O_2 partial pressure of the venous blood: $P_{\bar{V}O_2}=20$ and $P_{\bar{V}O_2}=40$ torr. Likewise, two cases for the CO_2 partial pressure of the venous blood have been taken as: $P_{\bar{V}CO_2}=45$ and $P_{\bar{V}CO_2}=55$ torr.

For both O_2 and CO_2 , in Figures 2A and 2C, increasing the capillary blood flow decreases the partial pressure variation along the length of the blood capillary. But for both gases, in Figures 2B and 2D, increasing blood flow increases the partial pressure variation along the length of the air capillary. An increased partial pressure gradient in the air capillary means that mass transport by diffusion is increased. So, when

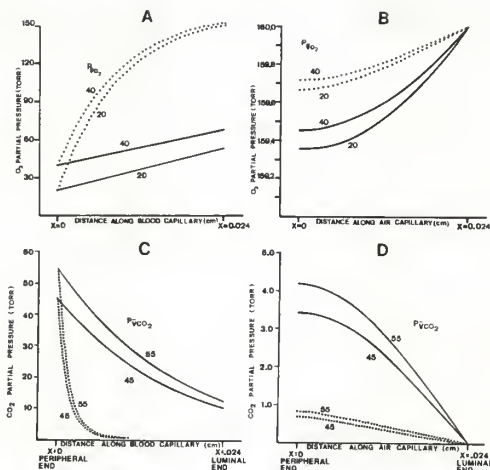


Figure 2. Partial pressures along a blood capillary and an air capillary when $\dot{Q}_p = 0.29$ ml/min (dotted lines) and $\dot{Q}_p = 2.9$ ml/min (solid lines). The cases considered for venous partial pressure are $P_{\bar{V}O_2} = 20$, $P_{\bar{V}O_2} = 40$, $P_{\bar{V}O_2} = 45$, and $P_{\bar{V}O_2} = 55$ torr. The luminal gas at the open end of the air capillary is described by $P_{O_2} = 160$ and $P_{CO_2} = 0$ torr. A: P_{O_2} along the blood capillary. B: P_{O_2} along the air capillary. C: P_{CO_2} along the blood capillary. D: P_{CO_2} along the air capillary.

the capillary blood flow increases, the exchange of O_2 and CO_2 between the blood phase and the parabronchial gas increases, even though the blood equilibration decreases.

When $P_{\bar{V}O_2}$ decreases without a change in capillary blood flow, a greater amount of O_2 is moved from the parabronchial gas into the blood. In Figures 2A and 2B this is shown by an increase in the partial pressure variation along both the air capillary and blood capillary. Likewise, Figures 2C and 2D show that when $P_{\bar{V}CO_2}$ increases without a change in capillary blood flow, the partial pressure variation increases along both the air capillary and blood capillary.

Comparison of Figures 2A and 2C shows that the capillary blood CO_2 partial pressure equilibrates more rapidly than the O_2 partial pressure. In alveolar lungs the rate at which pulmonary capillary blood equilibrates with alveolar gas depends upon the ratio of the diffusing capacity to the capacitance coefficient of blood (Forster, 1964; Wagner, 1977). This same ratio (see the definition of ρ in Appendices B and D) enters into the equations of Appendix B which describe the solution for partial pressure along a parabronchial blood capillary. Since the CO_2 diffusing capacity is larger than that of O_2 by a factor of 20, and the capacitance coefficient of CO_2 in blood is taken larger than that of O_2 by a factor of 3.36, the ratio of these quantities is larger for CO_2 than for O_2 by a factor of 5.95. Thus, the rate of exponential equilibration along the blood capillary is greater for CO_2 than for O_2 .

The variation in O_2 partial pressure along the length of the air capillary is less than one torr (Figure 2B) and the variation in CO_2 partial pressure is less than five torr (Figure 2D). For both O_2 and

CO_2 , the high \dot{Q}_p values and extreme parabronchial partial pressures have been chosen to give partial pressure variations along the air capillary which are near the maximum of the normal physiological range. The capillaries which experience conditions most nearly approaching these lie at the parabronchial entrance. The following capillaries along the parabronchus experience luminal gas which has already undergone some exchange. So the driving force for further gas exchange is reduced and the partial pressure variation along these air capillaries is less than that shown in 2B and 2D.

Figures 3A and 3B show that along the parabronchus from the entrance to the exit, the O_2 partial pressure decreases and the CO_2 partial pressure increases. There are two families of curves in both 3A and 3B. The family of dotted curves was computed from equations (47), (48), and (49) of Appendix B under the assumption of equal diffusion resistance in the air capillaries and the parabronchial lumen. The family of solid curves was computed under the assumption of bulk flow only in the parabronchial lumen (infinite diffusion resistance) and constant partial pressure along an air capillary (zero diffusion resistance).

In Figure 3 the parabronchial perfusion is $\dot{Q}_p = 0.29$ ml/min and the parabronchial ventilation varies from $\dot{V}_p = 0.022$ to $\dot{V}_p = 0.90$ ml/min. The state of venous blood is given by $P_{\bar{\text{VO}}_2} = 40$ and $P_{\bar{\text{VCO}}_2} = 45$ torr. The state of inspired gas is given by $P_{\text{iO}_2} = 160$ and $P_{\text{iCO}_2} = 0$ torr. The diffusion constants are $K_{\text{O}_2} = 6.28 \times 10^{-4}$ and $K_{\text{CO}_2} = 4.90 \times 10^{-4}$ mmol·min⁻¹·torr⁻¹·cm⁻¹.

The dotted curves, in which diffusion is accounted for, show a change in the partial pressure of the ventilating gas before it enters the parabronchus (region II). This is in contrast to the solid curves

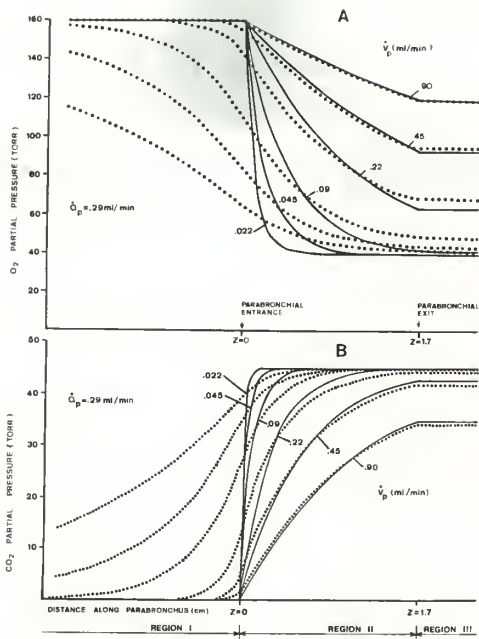


Figure 3. Partial pressures along the parabronchus computed under the assumption of (1): equal diffusion resistance in the air capillaries and parabronchial lumen (dotted curves) and, (2): constant partial pressure along the air capillaries and bulk flow only in the parabronchial lumen (solid curves). The parabronchial ventilation varies from $\dot{V}_p = 0.022$ to $\dot{V}_p = 0.90$ ml/min. The state of inspired gas is $P_{iO_2} = 160$ and $P_{iCO_2} = 0$ torr; the state of venous blood is $P_{\bar{V}O_2} = 40$ and $P_{\bar{V}CO_2} = 45$ torr. A: P_{O_2} along the parabronchus. B: P_{CO_2} along the parabronchus.

which neglect diffusion. Figure 3A shows that the partial pressure in the pre-parabronchial region decreases because O_2 diffuses out of this region into the parabronchus which has a lower O_2 partial pressure. Figure 3B shows that the partial pressure in the pre-parabronchial region increases because CO_2 diffuses backward into this region from the parabronchus which has a higher CO_2 partial pressure.

Figures 3A and 3B show that increasing the parabronchial ventilation causes the gas to equilibrate less fully with venous blood. At high ventilation rates the curves computed with parabronchial diffusion are closely approximated by the curves computed with bulk flow only. At lower ventilation rates this approximation no longer holds as diffusion becomes relatively more important in comparison with bulk flow.

The partial pressures computed with parabronchial diffusion show less change between the inspired and end-parabronchial values than do the partial pressures computed with bulk flow only. Depending on the ventilation rate, that change is less by factors as small as 0.94 and 0.98 for oxygen and carbon dioxide, respectively.

Comparison of 3A and 3B shows that at a fixed ventilation the rate of equilibration along the parabronchus is greater for CO_2 than for O_2 . This is a secondary consequence of the characteristics of gas exchange along a blood-air capillary pair. As shown in Figures 2B and 2D, at the parabronchial entrance the partial pressure gradient along the air capillaries is significantly greater for CO_2 than for O_2 . This implies that near the entrance there is more exchange of CO_2 between the air capillaries and the parabronchial lumen than there is of O_2 (also see Figure 4). This further implies that in the parabronchial lumen, CO_2 equilibrates faster than O_2 .

Figure 4 gives a more complete picture of the whole parabronchus as a gas exchange organ by combining the results describing partial pressure variation along the blood capillaries with those describing the variation along the parabronchial lumen. Results for O_2 are shown in 4A; for CO_2 in 4B. The series of curves on the left describes partial pressure variation in blood capillaries located at different positions along the parabronchus. In each capillary the partial pressure changes from the venous value to the end-capillary value. The rate and extent of that change depends on the partial pressure of the gas in the adjacent air capillary. The partial pressure in the air capillary depends upon the partial pressure in the parabronchial gas into which the air capillary opens, which in turn depends upon its location along the parabronchus. The variation in partial pressure of the gas along the parabronchus is shown by the curve on the right. The physical location of a blood capillary with respect to position along the parabronchus is indicated by the dotted lines. The vertical segment of the dotted line indicates the extent to which the capillary blood falls short of full equilibration with the gas in the adjacent air capillary. Gas leaving the parabronchus is at the partial pressure indicated by the right end point of the parabronchial gas curve. The partial pressure of arterial blood, formed from the blood emptying out of all the blood capillaries along the parabronchus, is an average of the values of partial pressure of the right end points of the blood capillary curves.

Figure 5 has been constructed in order to compare the rate of O_2 uptake (\dot{M}_{O_2}) to the rate of CO_2 elimination (\dot{M}_{CO_2}) by a single blood capillary. The computed quantities \dot{M}_{O_2} , \dot{M}_{CO_2} , and $\dot{M}_{CO_2}/\dot{M}_{O_2}$ (the respiratory exchange ratio) have been plotted against distance along the

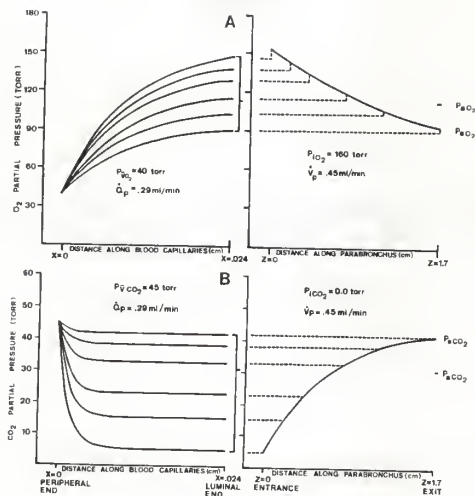


Figure 4. A: O_2 partial pressure along several parabronchial blood capillaries (left) and along the parabronchial lumen (right). The capillary location along the parabronchus is indicated by horizontal dotted lines. The extent to which blood falls short of full equilibration with air is indicated by vertical dotted lines. B: CO_2 partial pressure along several parabronchial blood capillaries and along the parabronchial lumen.

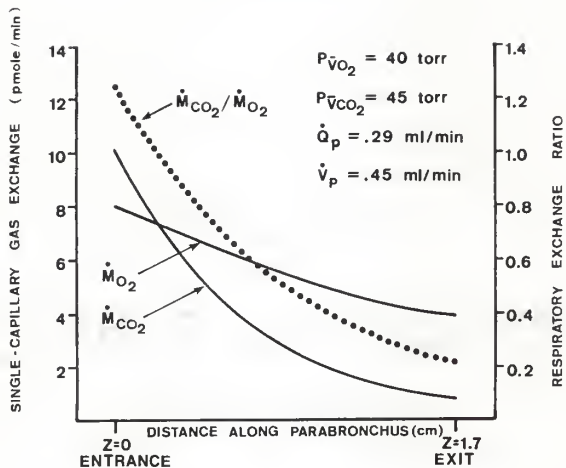


Figure 5. Gas exchange rate of CO_2 and O_2 by a single blood-air capillary pair plotted against distance along the parabronchus. Also shown is the ratio of these exchange rates.

parabronchus. In order to quantify the single capillary gas exchange rate, the number of blood-air capillary pairs per parabronchus has been taken to be 3.1×10^5 .

Since the capillaries near the parabronchial entrance experience the freshest gas and the following capillaries experience luminal gas which has already undergone some gas exchange, \dot{M}_{O_2} and \dot{M}_{CO_2} decrease along the parabronchus.

Figure 5 shows that \dot{M}_{CO_2} decreases faster than does \dot{M}_{O_2} , which causes the respiratory exchange ratio, $\dot{M}_{CO_2}/\dot{M}_{O_2}$, also to decrease along the parabronchus. It changes from 1.3 for the capillary pairs at the entrance to 0.21 for those at the exit. The over-all respiratory exchange ratio for this entire parabronchus is 0.61. This value is less than the expected value of about 0.8, probably because the model's use of a linear O_2 dissociation curve exaggerates the O_2 exchange.

DISCUSSION

The assumption of a linear dissociation curve is an approximation for the respiratory gases, oxygen and carbon dioxide. A consequence of the linear approximation for the sigmoid O_2 dissociation curve over the normal physiological range is an unrealistically high O_2 concentration in the blood when the O_2 partial pressure in the blood rises above about 100 torr. This implies an over-estimation of the O_2 absorbed, which further implies an over-estimation of the air capillary O_2 gradient. Therefore, the linear dissociation curve used here results in an exaggeration of the computed O_2 partial pressure variation along the air capillaries and along the parabronchus.

In contrast to O_2 , the effective CO_2 dissociation curve is well approximated by a straight line (Schiepers, Kawashiro, and Scheid, 1975).

A square velocity profile across the parabronchial lumen has been assumed in the calculations of partial pressure along the parabronchus. If the actual velocity profile deviates from this ideal, there will be additional mixing of gases in the lumen which is not accounted for. This implies an under-estimation of the effective diffusion in the curves of Figure 4.

Blood flows in the capillaries from the periphery of the parabronchus toward the lumen. In the air capillaries lying parallel to the blood capillaries, oxygen diffuses from the lumen toward the periphery and carbon dioxide diffuses from the periphery toward the lumen. This means that in the blood-air capillary network there are counter-current oxygen flows occurring simultaneously with co-current carbon dioxide flows.

In the parabronchus, the radial flow of capillary blood is perpendicular to the axial flow of luminal gas. Thus, the over-all parabronchial process can be described as cross-current gas exchange. The O_2 and CO_2 diffusive flows in the air capillaries, which are counter-current and co-current with respect to the O_2 and CO_2 bulk flows in the blood capillaries, move these gases between the cross-current flows of luminal gas and capillary blood.

Between the capillary blood and the parabronchial luminal gas there is a resistance to diffusion across the interface separating the blood phase from the gas phase and there is a resistance to diffusion through the gas phase of the air capillaries. We want to obtain an estimate of the relative importance of interface resistance to air capillary resistance within a single blood-air capillary pair. This estimate is obtained by evaluating the expression: $(P_{b,av} - P_{g,av}) / (P_{g,av} - P_{II})$. $P_{b,av}$ is an average partial pressure in the blood capillary; $P_{g,av}$ is an average partial pressure in the air capillary; P_{II} is the partial pressure at the luminal end of the air capillary. Partial pressures are taken as average at that point along the blood-air capillary pair where the gas exchange is half completed. The rationale behind this expression is that at a given rate of diffusive flow, the diffusion resistance between two points is proportional to their partial pressure difference.

Partial pressure values from the curves in Figure 2 have been used to evaluate the above expression. From 2A and 2B it is found that the resistance to O_2 uptake imposed by diffusion from the air capillary into the blood capillary is about 250 times the resistance imposed by diffusion through the air capillary for the four conditions: 1) $P_{\bar{V}O_2} = 20$ torr,

$\dot{Q}_p = 0.29$ ml/min; 2) $P_{\bar{V}O_2} = 40$ torr, $\dot{Q}_p = 0.29$ ml/min; 3) $P_{\bar{V}O_2} = 20$ torr, $\dot{Q}_p = 2.9$ ml/min; 4) $P_{\bar{V}O_2} = 40$ torr, $\dot{Q}_p = 2.9$ ml/min. From 2C and 2D it is found that the resistance to CO_2 excretion imposed by diffusion from the blood capillary into the air capillary is about 33 times the resistance imposed by diffusion through the air capillary for the two conditions: 1) $P_{\bar{V}CO_2} = 45$ torr, $\dot{Q}_p = 0.29$ ml/min; 2) $P_{\bar{V}CO_2} = 55$ torr, $\dot{Q}_p = 0.29$ ml/min. It is found to be about 8.5 for the other two conditions: 3) $P_{\bar{V}CO_2} = 45$ torr, $\dot{Q}_p = 2.9$ ml/min; 4) $P_{\bar{V}CO_2} = 55$ torr, $\dot{Q}_p = 2.9$ ml/min.

In contrast to the conclusions of Piiper and Scheid, 1977, these results show a difference between O_2 and CO_2 in the comparison of the importance of interface diffusion resistance to air capillary diffusion resistance to limit gas exchange. The principal reason for the difference between the two respiratory gases in this comparison is that the diffusing capacity of CO_2 across the blood-gas interface is 20 times greater than that of O_2 .

To find the relative importance of interface resistance to air capillary resistance for the whole parabronchus, it would be necessary to average the effects of all the blood-air capillary pairs along the entire length of the parabronchus.

The results shown in Figure 3 predict that the gas in the pre-parabronchial region will begin to show a reduction in O_2 partial pressure and an increase in CO_2 partial pressure before entering the parabronchus. This is due to forward diffusion of O_2 toward the parabronchus and backward diffusion of CO_2 from the parabronchus. Measurements of CO_2 partial pressure from the dorsobronchi of ducks, in which the ventilation is unidirectional during the respiratory cycle but variable

in flow rate (see for instance Scheid and Piiper, 1971), have been made by Jammes and Bouverot (1975). These measurements show phasic changes during the respiratory cycle, but the authors attribute these entirely to bulk movement of gas. Additional measurements will be necessary to determine the importance of backward diffusion on dorsobronchial CO_2 partial pressure during respiration in a live bird.

An assumption made by Scheid and Piiper (1970) in the analysis of their cross-current model was that the partial pressures of O_2 and CO_2 are constant throughout the gas phase of a cross section cutting the model parabronchus perpendicular to its axis. A second assumption made was the absence of any transport in the parabronchial lumen by diffusion in the axial direction. In the parabronchial model shown in Figure 1 the conditions of the first assumption are reached in the limit of an infinitely large diffusion constant for O_2 and CO_2 within the air capillaries. The conditions of the second assumption are reached in the limit of a zero valued diffusion constant for O_2 and CO_2 within the parabronchial lumen. Under these two limiting processes the solution for $P_{II}(z)$ (equation (48) in Appendix B), when evaluated at the parabronchial exit, reduces to equation (7) of Scheid and Piiper.

The results shown in Figure 2 support the reasonableness of the first simplifying assumption except for CO_2 in the neighborhood of the parabronchial entrance under conditions of high blood flow rate. The results shown in Figure 3 support the second simplifying assumption except under conditions of low ventilation rate.

APPENDIX A. The Differential Equations

Under the steady-state conditions in air capillary compartment n, the influx of the considered gas equals its efflux. This fact, together with the expressions of Figure 1B, leads to the equation

$$(1) \quad fK \left[\frac{P_{g,n+1} - P_{g,n}}{\Delta x} - \frac{P_{g,n} - P_{g,n-1}}{\Delta x} \right] = h(P_{g,n} - P_{b,n}) \Delta x.$$

Taking the limit $\Delta x \rightarrow 0$ in (1) yields the differential equation

$$(2) \quad fK \frac{d^2 P_g}{dx^2} = h(P_g - P_b).$$

Similar considerations applied to blood capillary compartment n lead to the differential equation

$$(3) \quad \beta q \frac{dP_b}{dx} = h(P_g - P_b).$$

Equating the left members of (2) and (3) yields

$$(4) \quad fK \frac{d^2 P_g}{dx^2} = \beta q \frac{dP_b}{dx}.$$

The boundary conditions on solutions of (2), (3), and (4) are imposed at the ends of the capillary pair. Both the closed end of the air capillary and the point at which venous blood enters the blood capillary lie on the parabronchial periphery at $x=0$. The open end of the air capillary and the point at which blood leaves the blood capillary lie on the parabronchial luminal surface at $x=l$. The boundary conditions are:

$$(5) \quad \text{at } x=0: \quad P_b(0) = P_v,$$

$$(6) \quad \text{at } x=0: \quad \left. \frac{dP_g}{dx} \right|_{x=0} = 0,$$

$$(7) \quad \text{at } x=l: \quad P_g(l) = P_{II}.$$

Boundary condition (6) results from the lack of diffusion across the end of the air capillary. Integration of (4) over the interval $[0, x]$ and application of the boundary conditions (5) and (6) yields

$$(8) \quad fK \frac{dP_g}{dx} - \beta q P_b = -\beta q P_v$$

Setting $x=l$ in (8), one obtains

$$(9) \quad fK \left. \frac{dP_g}{dx} \right|_{x=l} = \beta q (P_b(l) - P_v).$$

Either the right or left member of (9) describes the transport between a single air capillary and the parabronchus. The transport due to all the air capillaries opening into a single parabronchial compartment is obtained from the right hand side of (9) by replacing q with $(\dot{Q}_p \Delta z / L)$.

Assuming steady-state conditions for parabronchial compartment n (Figure 1C), equating the influx to the efflux, and taking the limit $\Delta z \rightarrow 0$, leads to the differential equation

$$(10) \quad \text{in region II:} \quad fK \frac{d^2 P}{dz^2} - \alpha \dot{V}_p \frac{dP}{dz} = \frac{\beta \dot{Q}_p}{L} (P_b(l) - P_v).$$

In regions I and III there is no gas exchange, so the differential equation to be satisfied is

$$(11) \quad \text{in regions I and III:} \quad fK \frac{d^2 P}{dz^2} - \alpha \dot{V}_p \frac{dP}{dz} = 0.$$

The boundary conditions to be satisfied by P_I , P_{II} , and P_{III} are:

$$(12) \quad \text{at } z \rightarrow -\infty: \quad P_I = P_1$$

$$(13) \quad \text{at } z=0: \quad P_I = P_{II},$$

$$(14) \quad \text{at } z=0: \quad \frac{dP_I}{dz} = \frac{dP_{II}}{dz},$$

$$(15) \quad \text{at } z=L : \quad P_{II} = P_{III} ,$$

$$(16) \quad \text{at } z=L : \quad \frac{dP_{II}}{dz} = \frac{dP_{III}}{dz} ,$$

$$(17) \quad \text{at } z>L : \quad \frac{dP_{III}}{dz} = 0 .$$

APPENDIX B. Solutions of Differential Equations

Next, the solutions for partial pressure along the blood and air capillaries are found. Taking the Laplace transforms of equations (3) and (8), one obtains two equations in the two unknowns P_g and P_b , which are the Laplace transforms of P_g and P_b , respectively. The two equations can be solved for P_g and P_b .

$$(18) \quad P_g = \frac{s + \rho}{s^2 + s\rho - \sigma} P_g(0) - \frac{\sigma}{s(s^2 + s\rho - \sigma)} P_V,$$

$$(19) \quad P_b = \frac{\rho}{s^2 + s\rho - \sigma} P_g(0) + \frac{s^2 - \sigma}{s(s^2 + s\rho - \sigma)} P_V,$$

where

$$(20) \quad \rho = \frac{h}{\beta q}, \quad \text{and} \quad \sigma = \frac{h}{fK}.$$

Taking inverse transforms of (18) and (19) yields solutions for P_g and P_b .

$$(21) \quad P_g(x) = H(x) P_g(0) + B(x) P_V.$$

$$(22) \quad P_b(x) = G(x) P_g(0) + D(x) P_V.$$

The functions $H(x)$, $B(x)$, $G(x)$, and $D(x)$ are given as follows.

$$(23) \quad H(x) = \frac{s_1 + \rho}{s_1 - s_2} e^{s_1 x} + \frac{s_2 + \rho}{s_2 - s_1} e^{s_2 x},$$

$$(24) \quad B(x) = 1 - \frac{\sigma}{s_1(s_1 - s_2)} e^{s_1 x} - \frac{\sigma}{s_2(s_2 - s_1)} e^{s_2 x},$$

$$(25) \quad G(x) = \frac{\rho}{s_1 - s_2} e^{s_1 x} + \frac{\rho}{s_2 - s_1} e^{s_2 x},$$

$$(26) \quad D(x) = 1 + \frac{s_1^2 - \sigma}{s_1(s_1 - s_2)} e^{s_1 x} + \frac{s_2^2 - \sigma}{s_2(s_2 - s_1)} e^{s_2 x},$$

where

$$(27) \quad s_1 = \frac{-\rho}{2} - \frac{1}{2} (\rho^2 + 4\sigma)^{1/2}, \quad \text{and} \quad s_2 = \frac{-\rho}{2} + \frac{1}{2} (\rho^2 + 4\sigma)^{1/2}.$$

A difficulty yet remaining with the solutions (21) and (22) is that they are given in terms of the pair of boundary values $P_g(0)$ and P_v instead of the pair P_{II} and P_v . To obtain the required form of the solutions, x is set equal to ℓ in equation (21). Then solving for $P_g(0)$ yields

$$(28) \quad P_g(0) = \frac{1}{H(\ell)} P_{II} - \frac{B(\ell)}{H(\ell)} P_v.$$

Substituting (28) into (21) and (22) gives the solutions for P_g and P_b in the form

$$(29) \quad P_g(x) = \frac{H(x)}{H(\ell)} P_{II} + [B(x) - \frac{H(x)B(\ell)}{H(\ell)}] P_v,$$

$$(30) \quad P_b(x) = \frac{G(x)}{H(\ell)} P_{II} + [D(x) - \frac{G(x)B(\ell)}{H(\ell)}] P_v.$$

Equations (29) and (30) are the desired solutions for partial pressure along the air and blood capillaries.

Next, the solutions for partial pressure along the parabronchus are found. From (30) one obtains

$$(31) \quad P_b(\ell) - P_v = \frac{G(\ell)}{H(\ell)} P_{II} + [D(\ell) - \frac{G(\ell)B(\ell)}{H(\ell)} - 1] P_v$$

Substitution of (31) into (10) yields the differential equation which must be satisfied in region II.

$$(32) \quad \frac{d^2 P}{dz^2} - \tau \frac{dP}{dz} - \psi P = \delta P_v.$$

The following substitutions have been made.

$$(33) \quad \tau = \frac{\alpha \dot{V}}{FK} P, \quad$$

$$(34) \quad \psi = \frac{\beta \dot{Q}_P}{FKL} \frac{G(\ell)}{H(\ell)} ,$$

$$(35) \quad \delta = \frac{\beta \dot{Q}_P}{FKL} [D(\ell) - \frac{G(\ell)B(\ell)}{H(\ell)} - 1] .$$

The solution of (32) is

$$(36) \quad P_{II}(z) = b_1 e^{t_1 z} + b_2 e^{t_2 z} - \frac{\delta}{\psi} P_V ,$$

where b_1 and b_2 are constants, and

$$(37) \quad t_1 = \frac{\tau}{2} - \frac{1}{2} (\tau^2 + 4\psi)^{1/2} , \quad \text{and} \quad t_2 = \frac{\tau}{2} + \frac{1}{2} (\tau^2 + 4\psi)^{1/2} .$$

The equation which must be satisfied in regions I and III is

$$(38) \quad \frac{d^2 P}{dz^2} - \tau \frac{dP}{dz} = 0 ,$$

where (33) has been combined with (11) to arrive at this form. The solutions of (38) for P_I and P_{III} are

$$(39) \quad P_I(z) = b_3 e^{\tau z} + b_4 ,$$

$$(40) \quad P_{III}(z) = b_5 e^{\tau z} + b_6 .$$

The constants b_1 - b_6 must be chosen so that the boundary conditions are satisfied. Substituting the solutions (36), (39), and (40) into boundary conditions (12)-(17) yields the following equations.

$$(41) \quad b_4 = P_i ,$$

$$(42) \quad b_3 + b_4 = b_1 + b_2 - \frac{\delta}{\psi} P_V ,$$

$$(43) \quad \tau b_3 = t_1 b_1 + t_2 b_2 ,$$

$$(44) \quad b_1 e^{t_1 L} + b_2 e^{t_2 L} - \frac{\delta}{\psi} P_V = b_5 e^{\tau L} + b_6 ,$$

$$(45) \quad t_1 b_1 e^{t_1 L} + t_2 b_2 e^{t_2 L} = \tau b_5 e^{\tau L} ,$$

$$(46) \quad b_5 = 0 .$$

Solving these equations for the b 's and substituting the resulting values into (36), (39), and (40) produces the desired solutions for P_I , P_{II} , and P_{III} .

$$(47) \quad P_I(z) = P_1 + \frac{t_1 t_2 e^{\tau z} (e^{t_2 L} - e^{t_1 L}) (P_1 + \frac{\delta}{\psi} P_V)}{t_1 e^{t_1 L} (t_2 - \tau) - t_2 e^{t_2 L} (t_1 - \tau)} ,$$

$$(48) \quad P_{II}(z) = -\frac{\delta}{\psi} P_V + \frac{\tau (t_2 e^{t_1 z + t_2 L} - t_1 e^{t_1 L + t_2 z}) (P_1 + \frac{\delta}{\psi} P_V)}{t_1 e^{t_1 L} (t_2 - \tau) - t_2 e^{t_2 L} (t_1 - \tau)} ,$$

$$(49) \quad P_{III}(z) = -\frac{\delta}{\psi} P_V + \frac{\tau (t_2 - t_1) e^{L(t_1 + t_2)} (P_1 + \frac{\delta}{\psi} P_V)}{t_1 e^{t_1 L} (t_2 - \tau) - t_2 e^{t_2 L} (t_1 - \tau)} .$$

APPENDIX C - Symbol Definitions

x	location along capillary (cm)
l	length of capillaries (cm)
f	cross-sectional area of air capillary (cm^2)
z	location along parabronchus (cm)
L	length of parabronchus (cm)
F	cross-sectional area of parabronchial lumen (cm^2)
h	diffusing capacity between blood and air capillaries per unit length ($\text{mmol} \cdot \text{min}^{-1} \cdot \text{torr}^{-1} \cdot \text{cm}^{-1}$)
K	Krogh's diffusion constant in gas phase ($\text{mmol} \cdot \text{min}^{-1} \cdot \text{torr}^{-1} \cdot \text{cm}^{-1}$)
β	capacitance coefficient in blood ($\text{mmol} \cdot \text{ml}^{-1} \cdot \text{torr}^{-1}$)
α	capacitance coefficient in gas phase ($\text{mmol} \cdot \text{ml}^{-1} \cdot \text{torr}^{-1}$)
q	blood supply to single blood capillary ($\text{ml} \cdot \text{min}^{-1}$)
\dot{Q}_p	blood supply to single parabronchus ($\text{ml} \cdot \text{min}^{-1}$)
\dot{V}_p	ventilation of single parabronchus ($\text{ml} \cdot \text{min}^{-1}$)
$P_{g,n}$	partial pressure in cell n of air capillary (torr)
$P_{b,n}$	partial pressure in cell n of blood capillary (torr)
P_g	partial pressure as a function of x in air capillary (torr)
P_b	partial pressure as a function of x in blood capillary (torr)
P_I, P_{II}, P_{III}	partial pressure as a function of z in region I, II, III (torr)
P_i	partial pressure of inspired gas (torr)
P_v	partial pressure of venous blood (torr)
s	Laplace transform variable
D_p	diffusing capacity of single parabronchus ($\text{mmol} \cdot \text{min}^{-1} \cdot \text{torr}^{-1}$)
A_p	cross sectional area of all air capillaries in a single parabronchus (cm^2)

APPENDIX D. Parameter Values

To obtain the parameter values used in evaluating the model results, the various quantities from different sources have been adjusted to fit a 1.6 kg bird.

King and Payne (1964) report the minute ventilation of resting chickens (3.4 kg, female) to be 766 ml/min. Vogel and Sturkie (1963) report the cardiac output of resting chickens (1.95 kg, female) to range from 234 ml/min (summer) to 345 ml/min (winter). From these data representative rates of ventilation and perfusion for a single parabronchus are found to be $\dot{V}_p = 0.45$ ml/min and $\dot{Q}_p = 0.29$ ml/min when the total number of parabronchi in both lungs is taken to be 800 (King and Cowie, 1969) and homogeneous distribution of blood and air among the parabronchi is assumed.

MacDonald (1970) gives ranges for the diameter of the parabronchial lumen (0.33-0.77 mm) and for the diameter of the parabronchial unit including the lumen and capillary network (0.77-1.26 mm) for the chicken (2 kg, female). Payne (1960) gives ranges for both the length of parabronchi (1.0-4.0 cm) and the diameter of parabronchial lumina (1.39-1.74 mm), also in chicken (2.90 kg, female). Based on these data, representative values have been selected as $\lambda = 2.42 \times 10^{-2}$ cm, $F = 4.58 \times 10^{-3}$ cm², $L = 1.7$ cm.

From the capacitance coefficient of O₂ and CO₂ in air ($\alpha = 5.87 \times 10^{-5}$ mmol·ml⁻¹·torr⁻¹), and the diffusion coefficients of O₂ (0.178 cm²·sec⁻¹, Handbook of Chemistry and Physics) and CO₂ (0.139 cm²·sec⁻¹, ibid) in air, the Krogh's constants of diffusion in the gas phase are determined to be $K_{O_2} = 6.28 \times 10^{-4}$ and $K_{CO_2} = 4.90 \times 10^{-4}$ mmol·min⁻¹·torr⁻¹·cm⁻¹.

From the O_2 and CO_2 dissociation curves of duck blood (Scheipers, Kawashiro, and Scheid, 1975) linear approximations have been taken as $\beta_{O_2} = 8.04 \times 10^{-5}$ and $\beta_{CO_2} = 27.0 \times 10^{-5} \text{ mmol} \cdot \text{ml}^{-1} \cdot \text{torr}^{-1}$.

To evaluate the solutions given by equations (29) and (30), it is necessary to evaluate ρ and σ (equation (20)). Multiplying the numerator and denominator of both these equations by the total number of air capillaries in a single parabronchus (see below) and the capillary length allows ρ and σ to be expressed as

$$\rho = \frac{D_p}{\beta \dot{Q}_p \ell}, \quad \text{and} \quad \sigma = \frac{D_p}{A_p K \ell}.$$

It remains to find D_p and A_p . Based on a carbon monoxide test Piiper, Pfeifer, and Scheid (1969) report the O_2 diffusing capacity in chicken (1.4 kg) to be $1.0 \text{ ml} \cdot \text{min}^{-1} \cdot \text{torr}^{-1}$. From this the O_2 diffusing capacity of the model parabronchus is selected as $D_{pO_2} = 6.38 \times 10^{-5} \text{ mmol} \cdot \text{min}^{-1} \cdot \text{torr}^{-1}$. The CO_2 diffusing capacity is taken to be twenty times as large: $D_{pCO_2} = 1.28 \times 10^{-3} \text{ mmol} \cdot \text{min}^{-1} \cdot \text{torr}^{-1}$.

Duncker (1972) reports the diameter of air capillaries in chicken to be $10 \mu\text{m}$ and also estimates that one half the volume of the blood-air capillary network is occupied by air capillaries. Based on these data, at a radius equal to 0.045 cm the total cross sectional area of all the air capillaries in a single parabronchus is estimated to be $A_p = 0.243 \text{ cm}^2$ and the total number of air capillaries in a single parabronchus is estimated to be 3.1×10^5 .

All the quantities necessary to evaluate the solutions have been assigned numerical values.

REFERENCES

- Abdalla, M. A., and A. S. King (1975). The functional anatomy of the pulmonary circulation of the domestic fowl. Respir. Physiol., 23:267-290.
- Dunker, H.-R. (1972). Structure of avian lungs. Respir. Physiol. 14:44-63.
- Forster, R. E. (1964). Diffusion of Gases. In: Handbook of Physiology Respiration. Washington, D.C.: Am. Physiol. Soc., 1964, Sect. 3, Vol. 1, p. 839-872.
- Jammes, Y., and P. Bouverot. (1975). Direct P_{CO_2} Measurements in the dorso-bronchial gas of awake peking ducks: evidence for a physiological role of the neopulma in respiratory gas exchanges. Comp. Biochem. Physiol. 52A:635-637.
- King, A. S., and D. C. Payne (1964). Normal breathing and the effects of posture in Gallus Domesticus. J. Physiol. (London). 174:340.
- King, A. S., and A. F. Cowie (1969). The functional anatomy of the bronchial muscle of the bird. J. Anat. 105:323-336.
- MacDonald, J. W. (1970). Observations on the histology of the lung of Gallus Domesticus. Br. Vet. J. 126:89-93.
- Payne, D. C. (1960). Observations of the functional anatomy of the lungs and air sacs of Gallus Domesticus. Ph.D. Thesis, University of Bristol, Bristol, England.
- Piiper, J., K. Pfeifer, and P. Scheid (1969). Carbon monoxide diffusing capacity of the respiratory system in the domestic fowl. Respir. Physiol. 6:309-317.
- Piiper, J., and P. Scheid. (1977). Diffusion within parabronchial air capillaries as a limiting factor for pulmonary gas exchange in birds. J. Physiol., London. 270:66P-67P.
- Scheid, P., and J. Piiper (1970). Analysis of gas exchange in the avian lung: Theory and experiments in the domestic fowl. Respir. Physiol. 9:246-262.
- Scheid, P., and J. Piiper. (1971). Direct measurement of the pathway of respired gas in duck lungs. Respir. Physiol. 11:308-314.
- Scheipers, G., T. Kawashiro, and P. Scheid (1975). Oxygen and carbon dioxide dissociation of duck blood. Respir. Physiol. 24:1-13.

- Vogel, J. A., and P. D. Sturkie (1963). Cardiovascular responses on chicken to seasonal and induced temperature changes. Science. 140:1404.
- Wagner, P. D. (1977). Diffusion and chemical reaction in pulmonary gas exchange. Physiol. Rev. 57:257-312.
- West, N. H., O. S. Bamford, and D. R. Jones. (1977). A scanning electron microscope study of the microvasculature of the avian lung. Cell Tiss. Res. 176:553-564.
- Zeuthen, E. (1942). The ventilation of the respiratory tract in birds. Kgl. Danske Videnskab. Selskab. Biol. Medd. 17:1-51.

THEORY OF GAS EXCHANGE IN THE AVIAN LUNG

by

WILLIAM DAVID CRANK

B.S., Kansas State University, 1968

AN ABSTRACT OF A MASTER'S THESIS

submitted in partial fulfillment of the

requirements for the degree

MASTER OF SCIENCE

Department of Electrical Engineering

KANSAS STATE UNIVERSITY
Manhattan, Kansas

1978

To understand the distribution of oxygen and carbon dioxide in the avian lung, a theoretical treatment of gas exchange in the parabronchus of the avian lung is described. The model used is modified after Zeuthen (1942). Cases which treat diffusion through the air capillaries, diffusion through the parabronchial lumen, and diffusion through both these spaces are considered. In these cases the O_2 dissociation curve is approximated by a straight line. Another case has been considered in which diffusion through the air spaces is neglected, but the O_2 dissociation curve is more accurately approximated by a polynomial. The relationship of the partial pressures of O_2 and CO_2 within the blood capillaries, air capillaries, and parabronchial lumen to parabronchial blood flow and ventilation is graphically shown.

The results indicate that the maximum partial pressure variations of O_2 and CO_2 along the length of an air capillary are less than one torr and five torr, respectively. Also, the resistance to gas exchange imposed by diffusion across the blood-gas interface is many times greater (about 250 times greater for O_2 ; from 8.5 to 33 times greater for CO_2) than the resistance imposed by diffusion through the air capillaries. The assumption of bulk flow only through the parabronchial lumen yields accurate results at resting and high ventilation rates, but axial diffusion in the lumen must additionally be considered at lower ventilation rates. Before entering the parabronchus, the gas in the pre-parabronchial region shows a reduction in O_2 partial pressure due to forward diffusion toward the parabronchus and an increase in CO_2 partial pressure due to backward diffusion from the parabronchus.